LAPPEENRANTA UNIVERSITY OF TECHNOLOGY
Faculty of Technology
Degree Programme in Electrical Engineering

Juho Montonen

FIELD WEAKENING, PARAMETERS AND OPERATION RANGE OF THE PERMANENT MAGNET TRACTION MOTORS

Examiners: Professor Juha Pyrhönen
D.Sc. Pia Lindh

ABSTRACT

Lappeenranta University of Technology
Faculty of Technology
Degree Programme in Electrical Engineering

Juho Montonen
Field Weakening, Parameters and Operation Range of the Permanent Magnet Traction Motors

2011

Master's Thesis.
74 pages, 35 figures, 1 appendix

Examiners: Professor Juha Pyrhönen, D.Sc. Pia Lindh

Keywords: field weakening, permanent magnet synchronous machine

The main focus of this thesis is to define the field weakening point of permanent magnet synchronous machine with embedded magnets in traction applications. Along with the thesis a modelling program is made to help the designer to define the field weakening point in practical applications.

The thesis utilizes the equations based on the current angle. These equations can be derived from the vector diagram of permanent magnet synchronous machine. The design parameters of the machine are: The maximum rotational speed, saliency ratio, maximum induced voltage and characteristic current.

The main result of the thesis is finding out the rated rotational speed, from which the field weakening starts. The action of the machine is estimated at a wide speed range and the changes of machine parameters are examined.

TIIVISTELMÄ

Lappeenrannan teknillinen yliopisto
Teknillinen tiedekunta
Sähkötekniikan koulutusohjelma

Juho Montonen
Kestomagneettitahtikoneen kentänheikennys, parametrit ja toiminta-alue ajoneuvosovelluksissa

2011

Diplomityö
74 sivua, 35 kuvaa, 1 liite

Tarkastajat: professori Juha Pyrhönen, tohtori Pia Lindh

Hakusanat: kentänheikennys, kestomagneettitahtikone

Diplomityön päätavoitteena on määrittää ajoneuvosovelluksissa käytettävän kestomagneettitahtikoneen kentänheikennyspiste kun koneessa esiintyy reluktanssivääntömomenttia. Työn ohessa laaditaan ohjelmakokonaisuus, jonka avulla kentänheikennyspisteen määritys onnistuu.

Työ toteutetaan käyttämällä virtakulmaan perustuvia yhtälöitä, jotka ovat johdettavissa kestomagneettitahtikoneen vektoripiirroksesta. Koneen suunnitteluparametreiksi valitaan maksimipyörimisnopeus, induktanssisuhde, indusoituneen jännitteen huippuarvo sekä karakteristinen virta.

Työn lopputuloksena määritetään nimellispyörimisnopeus, josta kentänheikennys alkaa. Diplomityössä arvioidaan koneen toimintaa laajalla pyörimisnopeusalueella ja tarkastellaan koneen parametrien muutoksia suunnitteluparametreja muutettaessa.

PREFACE

This master thesis is made in the Lappeenranta University of Technology at the department of electric engineering and the work is part of the FiDiPro project. Professor Juha Pyrhönen has been the first examiner and also the director of this work. I want to thank him for an interesting subject and the support that he has given me all these years during my studies. I thank also for Ph. D. Pia Lindh for working as a second examiner.

I also want to thank Professor Juan A. Tapia-Ladino for the guidelines he has given me through this work. His advices have been a good help to find the solutions to this thesis.

I want to thank my parents Pauli and Marjaleena for giving me good basis of life and the help that they have given me during my study. Special thanks to my siblings Miika and Laura and of course thanks to Ari, too.

And for Anita thank you for being the love and the light of my life and for your continuous support through the past year because it was not the easiest one for me.

In Reykjavik 18.9.2011

Juho Montonen

TABLE OF CONTENTS

ABBREVIATIONS AND SYMBOLS

PM	permanent magnet
DC	direct current
AC	alternating current
PMSM	permanent magnet synchronous machine
EMF	electromotive force
MTPA	maximum torque per ampere
MTPV	maximum torque per volt
DTC	direct torque control
AlNiCo	aluminium nickel cobalt
SmCo	samarium cobalt
NdFeBo	Neodymium Iron Boron
pu	per unit
SynRaPMSM	Synchronous reluctance assisted permanent magnet synchronous machine

Roman letters

$\boldsymbol{a}$	phase shift operator $e^{j2\pi/3}$
B	magnetic flux density [Vs/m^2], [T]
$BH_{\max}$	maximum energy product
B_{r}	remanent flux density [T]
e_{m}	air gap flux induced voltage [V]
E_{PM}	permanent magnet induced voltage [V]
e_{s}	induced voltage of the stator [V]
f	frequency [Hz]
$f_{\mathrm{fwp,limit}}$	upper limit for the field weakening range [Hz]
f_{n}	nominal frequency [Hz]
H	magnetic field strength [A/m]
H_{cB}	normal coercivity
H_{cJ}	intrinsic coercivity
i_{d}	direct axis current in the rotor reference frame [A]
i_{D}	direct axis damper winding current [A]
i_{dref}	direct axis reference current [A]
i_{md}	direct axis magnetizing current [A]
i_{mq}	quadrature axis magnetizing current [A]
I_{n}	nominal current [A]

i_{PM}	field current [A]
i_q	quadrature axis current in rotor reference frame [A]
i_Q	quadrature damper winding current [A]
i_{qref}	quadrature axis reference current [A]
$\boldsymbol{i_s}$	stator current vector [A]
$i_{s,meas}$	measured stator current [A]
i_{sref}	stator current reference [A]
I_x	characteristic current [A]
J	magnetic polarization [Vs/m^2]
K_{sk}	skewing factor
L	inductance [Vs/A], [H]
L_d	direct axis synchronous inductance [H]
L_{md}	direct axis magnetizing inductance [H]
L_{mq}	quadrature axis magnetizing inductance [H]
L_q	quadrature axis synchronous inductance [H]
$L_{s\sigma}$	stator stray inductance [H]
m	number of phases
N	number of coil turns
n	rotation speed [rpm]
p	number of pole pairs
P_J	Joule losses [W]
q	number of slots per pole and phase
R_m	reluctance [A/Vs]
R_s	stator resistance [Ω]
T	torque [Nm]
T_{max}	maximum torque [Nm]
u_{ph}	phase voltage [V]
$\boldsymbol{u_s}$	stator voltage vector
$u_{s,est}$	estimate of the stator voltage [V]
u_{sd}	direct axis stator voltage [V]
u_{sq}	quadrature axis stator voltage [V]

Greek letters

γ	current angle
δ	load angle
α	electrical skew angle
β	current phase angle

θ	rotor angle in stator reference frame
μ_r	relative permeability
ξ	winding factor
ρ	resistivity [Ωm]
Φ	magnet flux [Vs]
φ	power angle
ω	angular frequency [rad/s]
Ω	mechanical angular speed [rad/s]
ω_max	maximum angular frequency [rad/s]
Ω_max	maximum mechanical angular speed [rad/s]
ω_s	angular frequency of the stator flux [rad/s]
ψ_md	direct axis flux linkage of the airgap [Vs]
ψ_mq	quadrature axis flux linkage of the airgap[Vs]
ψ_PM	flux linkage of the airgap [Vs]
ψ_s	stator flux linkage [Vs]
$\psi_\mathrm{s,est}$	estimate of stator flux [Vs]
ψ_sd	direct axis flux linkage [Vs]
ψ_sq	quadrature axis flux linkage [Vs]
$\boldsymbol{\psi_s}$	flux linkage vector [Vs]

Sub- and superscripts

D	direct axis damper current
d	direct axis of stator parameters in rotor reference frame
DC	direct-(current,voltage)
FW	field weakening
fwp	field weakening point
J	Joule
lim	limit
m	magnetizing-
max	maximum
meas	measured
MTPA	maximum torque per ampere
MTPV	maximum torque per volt
n	nominal, rated
ph	phase
PM	permanent magnet

q	quadrature axis of stator parameters in rotor reference frame
Q	quadrature damper current
r	rotor, superscript rotor reference frame
ref	reference
s	stator, superscript stator reference frame
sk	skew
σ	leakage
A,B,C,N	phases

1. INTRODUCTION

In the future electrical drives will become the key technology in vehicles and work machines. Asynchronous machines seem to live their golden era and different kinds of synchronous machines claim the field of electrical machines. One of the most important machines is nowadays the permanent magnet synchronous machine. The permanent magnet (PM) technology is a fast emerging technology also in traction applications, similarly as in wind power, nowadays. This kind of machine seems to find its place in every application. The permanent magnet synchronous machine (PMSM) has taken the place of other machines because it can be made more compact and smaller and it can still be as efficient as other machines, and even more efficient.

PMSM can be constructed by either embedding the magnets in the rotor core or by placing them on the rotor surface. Particularly, permanent magnet machines with embedded magnets will be studied in this thesis but the methods will suit also surface magnet machines as well as interior permanent magnet machines.

PMSM with embedded magnets can have a good performance in the field weakening range. However, the field weakening operation can be difficult in a permanent magnet machine drive because the permanent magnets create their own fixed fluxes. The power capability over a wide speed range is also a topic, which needs investigation.

The typical traction motor properties which are, in particular, needed are a wide speed region and a very high starting torque. The motor power requirement continuously changes with time depending on the road conditions and driving schedules, and that is why the extended speed range is extremely important for variable speed traction applications (Hall & Balda 2002). In city traffic the high starting torque is needed but in highway traffic a wide speed range is needed.

The field weakening range operation is perhaps the most essential thing in the permanent magnet machine drives which are used in traction applications because when the wanted speed is achieved it is more economical and energy efficient to drive the machine with a lower torque. To exploit the full torque and power potential of the drive during field weakening, an operation at or very close to the voltage limit is compulsory.

During the drive design process it is essential to find a good match between the converter current capabilities and the motor torque capabilities. In traction drives, normally a two to three times the motor rated torque is needed in starting and correspondingly two or more times the base speed is needed in the speed range. This work studies in details the torque and speed range capabilities of the PMSM in converter control.

1.1 Characteristics of the traction motors

The permanent magnet synchronous machines are a natural choice to the traction applications because in traction the most important requirements are reliability, lightness and durability. The PMSM is a good choice to fill all these requirements. The permanent magnet machine has some great advantages and it is the best machine in many ways for the traction applications. These main advantages are

- Highest possible power density
- High efficiency
- Reliability
- Low cogging torque
- High starting torque
- Chance to get torque in very high speed region

Nowadays, machines in the traction applications are often synchronous reluctance assisted permanent magnet motors with interior magnets. The rotor with V-shape magnets have been used in the hybrid electric machines quite much. This kind of a machine produces a significant amount of reluctance torque and the total performance is good. The field weakening properties of the machine type form the great advantage of that kind of machine structure. In traction applications it is the directional factor because a motor needs to produce different amounts of torque depending on the speed. The traction motor should be designed for high torque low speed operation, high efficiency nominal speed operation and a wide field weakening range to attain very high speeds.

When the machine is designed there are expectation of good performance, high efficiency and high reliability. The machine must be also economical in terms of cost, weight and size. That can lead to problems with the field weakening to have an efficient and at the same time an economical machine. It is very difficult to get all the previous properties in the same machine at the same time.

1.2 Hybrid electric vehicle

Let us present next the basics of the hybrid vehicles shortly because the machines that this thesis will handle are used in traction applications. The term hybrid electric vehicle means that it is the combination of internal combustion engine and one or more electrical machines. A low emissions and energy efficiency are the driving forces to move in hybrid and full electric vehicles in the future instead of internal combustion engine. Also oil shortage and the high prices of gasoline are the reasons why old internal combustion engines need to be replaced with electric machines. Because cars and other vehicles are one of the main sources of air pollution, they need to be replaced with hybrid vehicles.

There are many types of hybrid electric vehicles which are divided for example by the power between power sources. These types are parallel, series and series-parallel-hybrids. The parallel hybrid means that internal combustion engine and electric machine are both connected to a mechanical and magnetic transmission. One electric machine is needed in the parallel hybrid and it works both as a motor and as a generator.

The series hybrid vehicles are driven only by electric traction applications. The electric machines have a high power to weight ratio and these machines in the series hybrid vehicles can provide torque over a very large speed range. In that hybrid type the internal combustion engines are used to drive an electric generator instead of directly driven the wheels of the vehicle and hence the generator is providing the power to the electric motors (Chizh 2010, 17-18).

The series-parallel hybrids can be driven only with engines or only with batteries or a combination of both. That is why that series-parallel hybrid type is usually called a full hybrid. In that kind of electric drive there is one electric machine and one internal combustion engine. These drives are often equipped with planetary gearbox and the electric machine can run on as a generator charging the batteries.

These hybrid types will not be studied further more in this thesis but they are just shortly described just to remind of what kind of hybrid types which are divided by the power between power sources, there is.

1.3 Motivation and goal of the thesis

It is important to study this subject because electric and hybrid vehicles will become more common in the future. Low emissions and energy efficiency are the driving forces to move in hybrid and full electric vehicles in the future instead of internal combustion engine. In

variable speed drives, this kind of permanent magnet synchronous machine can save the energy and provide better and optimal control over the whole process.

The main point of this thesis is to study, when the machine moves in the field weakening range and how the stator flux is controlled in every operation point. Basically this work studies how to define the field weakening point in permanent magnet machines which are used in traction applications.

This work concentrates and limits only to study the field weakening process of permanent magnet synchronous machines and hence equations and methods which are used during this work, cannot be used with other machine types.

1.4 Organization of the thesis

The analysis of this work is divided so that in chapter 2 the construction and the mathematical model of permanent magnet synchronous machine are presented. Control methods of PMSM are considered in chapter 3. In chapter 4 the basics of the field weakening process, losses of the machine and saturation model are studied. The purpose of chapter 5 is to present the modelling of the program which solves the field weakening point of the machine and in chapter 6 the results of the program is presented. Conclusions and summary of this thesis is collected in chapter 7.

2. PERMANENT MAGNET MACHINE

The permanent magnet synchronous machine is a synchronous machine whose characteristics are improved with permanent magnets. At the moment there are very many different PM machine types. Basically these machines can be divided into two categories: PMSMs with saliency and non-salient PMSMs. A PMSM with saliency has the inductance ratio L_q / $L_d > 1$ when the non-salient pole PMSM has L_q / $L_d \approx 1$. In permanent magnet synchronous machines with embedded magnets the direct axis inductance L_d is usually smaller than the quadrature axis inductance L_q because the direct axis armature reaction magnet flux path contains the very low permeability permanent magnets and the quadrature axis magnet flux path in the rotor flows mostly in iron. In rotor surface magnet machines the q-axis armature reaction flux travels under the magnets and in interior magnet machines the flux travels correspondingly over the magnets (Schiferl and Lipo 1990, 116). Figure 1 illustrates the PMSM family.

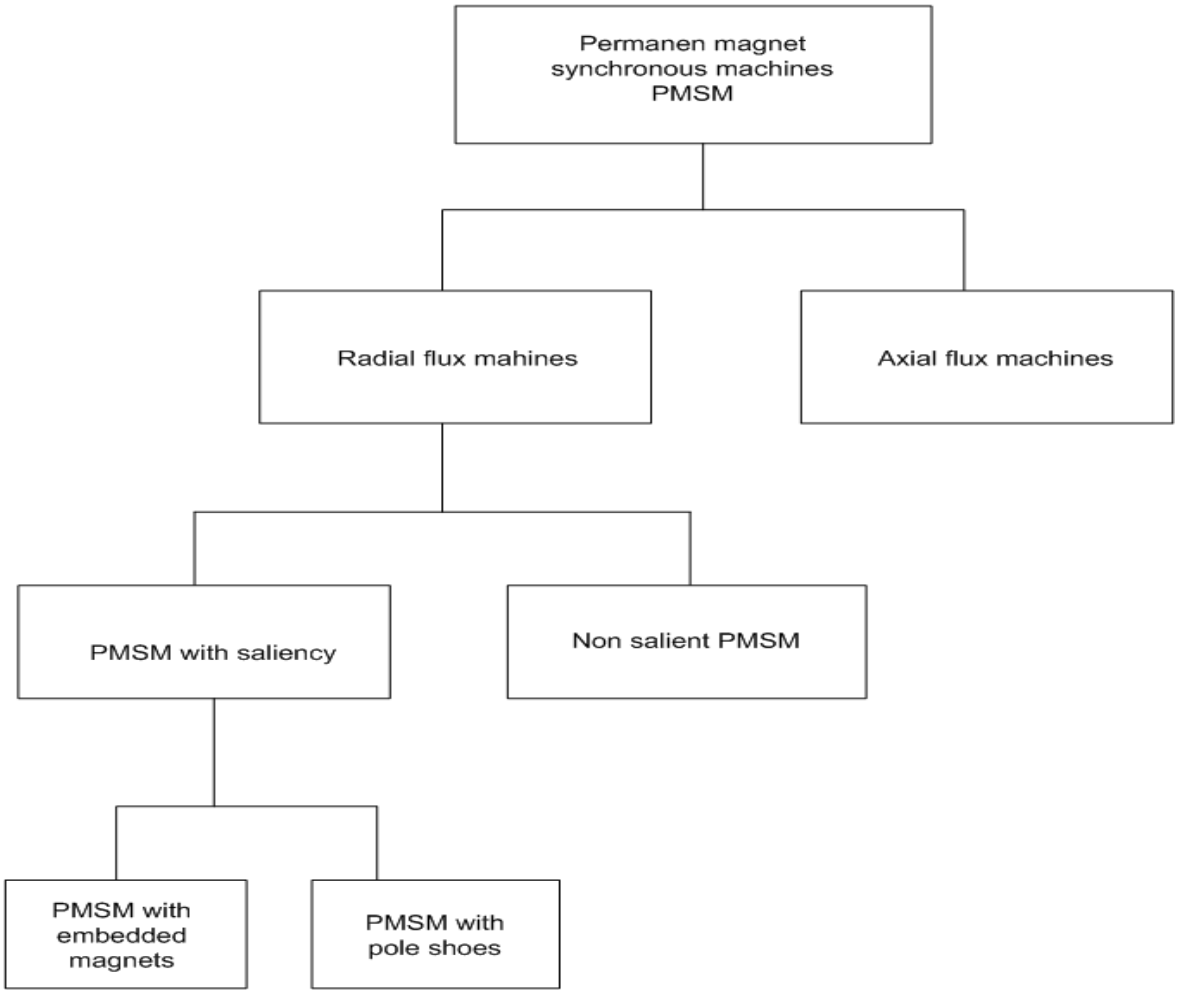

Figure 1 PMSM-family

In figure 1 it can be seen that the PMSMs with saliency can be divided in PMSMs with embedded magnets and PMSMs with pole shoes. There is also an own machine type; the axial flux machine which seems to be one of the trendsetters in traction applications at the moment. The axial flux machine can, at least in principle, be divided into similar subcategories as the radial flux machine.

Nowadays, there has been lot of interest in the use of permanent magnet synchronous reluctance motors in the field weakening applications such as traction which require a wide constant power speed range. The permanent magnet assisted synchronous reluctance machine has the saliency-based reluctance torque as its main torque producing method and the permanent magnets mainly help in improving the reluctance machine characteristics. This machine type is mainly limited to low pole pair numbers (in practice p = 2 or p = 3) guaranteeing a high saliency. If the permanent magnet torque, however, is the main torque we could call the machine – vice versa – the synchronous reluctance assisted permanent magnet machines (SynRaPMSMs) which have excellent properties also in cases of multiple pole designs and have good abilities to control the stator flux in the field weakening operation. These machines have a lower saliency than the previous type but are more suitable in high torque applications. Multiple pole arrangements can guarantee very lightweight high torque machine designs as the machine yokes can be made thin. The saliency, however suffers when the pole pair number gets high and, therefore, the permanent magnet based torque dominates in these machines being otherwise theoretically quite similar as the permanent magnet assisted synchronous reluctance machines.

The machines with embedded magnets (interior magnet machines) have saliency and, therefore, have some advantages compared to rotor surface magnet machines in traction applications. They have better control properties and also higher torque at the lowest speeds (Lindh et al. 2011).

The interior PM machine produces excitation torque caused by the PM interaction with the quadrature axis current and reluctance torque caused by the rotor saliency. The reluctance torque is created with the inductance difference between the direct (d) axis and quadrature (q) axis. The reluctance torque component can improve the torque capability significantly, especially, at low and high speeds. The rotor surface magnet machine does not have inductance difference at all, and therefore, there is no reluctance torque available. The field weakening is difficult with such a machine. The interior PM machine can have better overload conditions than the rotor surface PM machine.

There has been a lot of discussion about the stator windings in traction motors. Traditional distributed stator windings with the number of slot per pole and phase $q \geq 1$ are widely used. The stator has, with that kind of winding relatively low ratio of leakage to magnetizing inductance which makes it possible to reach high saliency ratios (Soong(a) et al. 2007).

The other widely used stator winding type is the concentrated tooth windings which are wrapped around the stator teeth. With concentrated windings the number of slots per pole and phase is typically $q \leq 0.5$. The concentrated windings have the high ratios of leakage to magnetizing inductance. This is very useful, when one wants to increase the stator inductance. Increasing of the stator inductance will reduce the achievable saliency ratio. Manufacturing of the stator is much easier with concentrated windings. The concentrated windings also offer good thermal performance. With concentrated windings in the stator, the rotor surface PM machine has been shown to produce remarkably good field weakening performance (Soong(a) et al. 2007).

2.1 Axial flux machine

The axial flux machine can be constructed with two stators and one rotor or the other way around. There are many investigations and new constructions are emerging every now and then about the axial flux machines. With the axial flux machine there are some advantages. It can be smaller and more compact than normal radial flux PMSM. Axial flux PMSMs can be used in applications where short axial length is needed and therefore axial flux PMSMs are common in hybrid vehicles. Axial-flux PMSMs can be designed for a higher torque-to-weight ratio than the radial flux machines. The other advantages of an axial-flux machine are lower noise and vibration levels and better efficiency (Aydin et al. 2010).

The drawback of axial-flux machine is the area of field weakening. Of course the mechanical design of the axial-flux machine can also be complicated because the end windings of the stator are close to the rotor shaft and that can be problematic. The manufacturing of the stator is more difficult than in radial flux machines because of the variable stator slot pitch as a function of the radial position of the lamination. However, in mass series production the stator of an axial-flux machine is cheaper than the stator of a corresponding radial flux machine because it needs less lamination material. Eddy current losses of axial-flux PMSM can damage the PM material in the rotor and the probability of demagneti-

zation is high during short circuit (Chizh 2010). Figure 2 illustrates the structure of an axial-flux machine with two rotors and one stator.

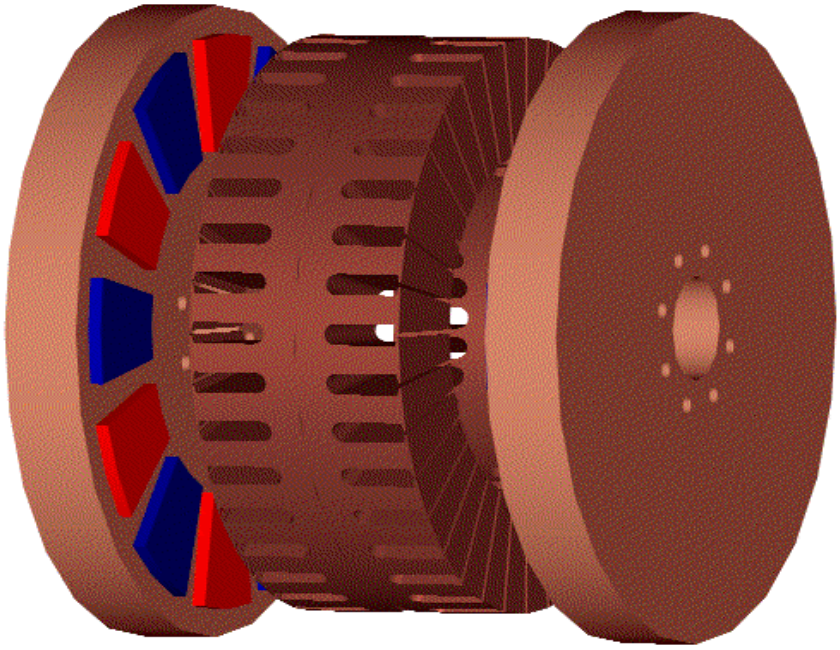

Figure 2 Rotor surface magnet two-rotors-single-stator structure (Parviainen 2005)

Figure 2 shows one of the structures of axial-flux machines. With this kind of structure, the efficiency can be improved and also the power density of the machine is getting better. Of course, mechanical problems are evident as there seems to be no space to support the stator. Other common structures of the axial-flux machine are the single-rotor-single-stator construction, the single-rotor-two-stators and the multistage structure including two stator blocks and three rotor blocks (Parviainen 2005).

In the two-stator-single-rotor machine structure the rotor can be made totally without iron. Then the rotor body is fully constructed with e.g. glass fibre.

The axial-flux machines are widely used as hybrid traction motors and as generators, however, this machine type will no longer be studied in this thesis because the main area of interest is the machine general behaviour in the operating range depending on the machine parameters.

2.2 Permanent magnet materials in PMSM

In the beginning one needs to take a look at which permanent magnet materials are used in the permanent magnet synchronous machines. The history of the permanent magnets which are used in the permanent magnet motors starts in the 20th century. The first important magnets were AlNiCo magnets which were discovered in the late 1930's. The use of these magnets is still common in many applications because of their high remanent flux density, high operating temperatures, good temperature stability and good corrosion resistance (Ruoho 2011). However, in motors the use is very difficult because of the low coercive force.

After AlNiCo magnets the material that was discovered was a ferrite magnet. The disadvantage of ferrites is that they have relatively low remanent flux density. The hard ferrites have low cost and for that reason they are widely used in many applications. The ferrites do not conduct electricity which gives for them good properties for many applications (Ruoho 2011). Hard ferrites have relative permeability in the range of 1.3 which means that in case of rotor surface magnets there will be some saliency in the motors.

After ferrites, in the seventies, the rare earth magnets were discovered. Then such magnets as $SmCo_5$ and Sm_2Co_{17} were introduced. Both these magnets have relatively high remanence, high maximum operating temperatures and high corrosion resistance. SmCo magnets are expensive because of the high price of cobalt. The main reason for that is why SmCo magnets are still used in machines nevertheless their prices is the high maximum operating temperature. Any other magnet material has not such high temperature endurance.

The newest magnet material was discovered in 1983 (Pyrhönen 2008). The material is NdFeB, which has higher remanent flux density than any other present day permanent magnet material. The disadvantage of the NdFeB magnet is that it cannot tolerate as high temperatures as the SmCo or the AlNiCo magnets. The NdFeB magnets have a largely linear demagnetizing behaviour but they have one big disadvantage. They are vulnerable to corrosion which means that the magnets must be protected by coating in many applications. The NdFeB magnets are also very fragile and they must be handled very carefully. This material is, however, nowadays the most used permanent magnet material in the PMSMs and since the introduction of the NdFeB, the use of the permanent magnet machines has risen in the new level. The NdFeB improves motor efficiency remarkably and gives a possibility to reach a high power density machine. Neo-magnets have a very low relative permeability, in the range of 1.03 which means that, in practice a machine with rotor surface Neo-magnets has almost no saliency.

The magnetic properties of the permanent magnet material are normally presented with hysteresis curves. The properties that are needed at magnet material in the permanent magnet machine are (Pyrhönen 2008):

- Remanence B_r
- Intrinsic coercivity H_cJ and normal coercivity H_cB
- Relative permeability μ_r
- Resistivity ρ
- Squareness of the polarization hysteresis curve
- The maximum energy product BH_max
- Mechanical characteristics
- Chemical characteristics

The hysteresis curve contains two different curves: *BH* curve and *JH* curve. The first mentioned curve describes the flux density B through the magnet as a function of the external magnetic field strength H. The second mentioned curve describes the magnetic polarization J as a function of the external magnetic field strength H. An example of a hysteresis curve is shown in figure 3.

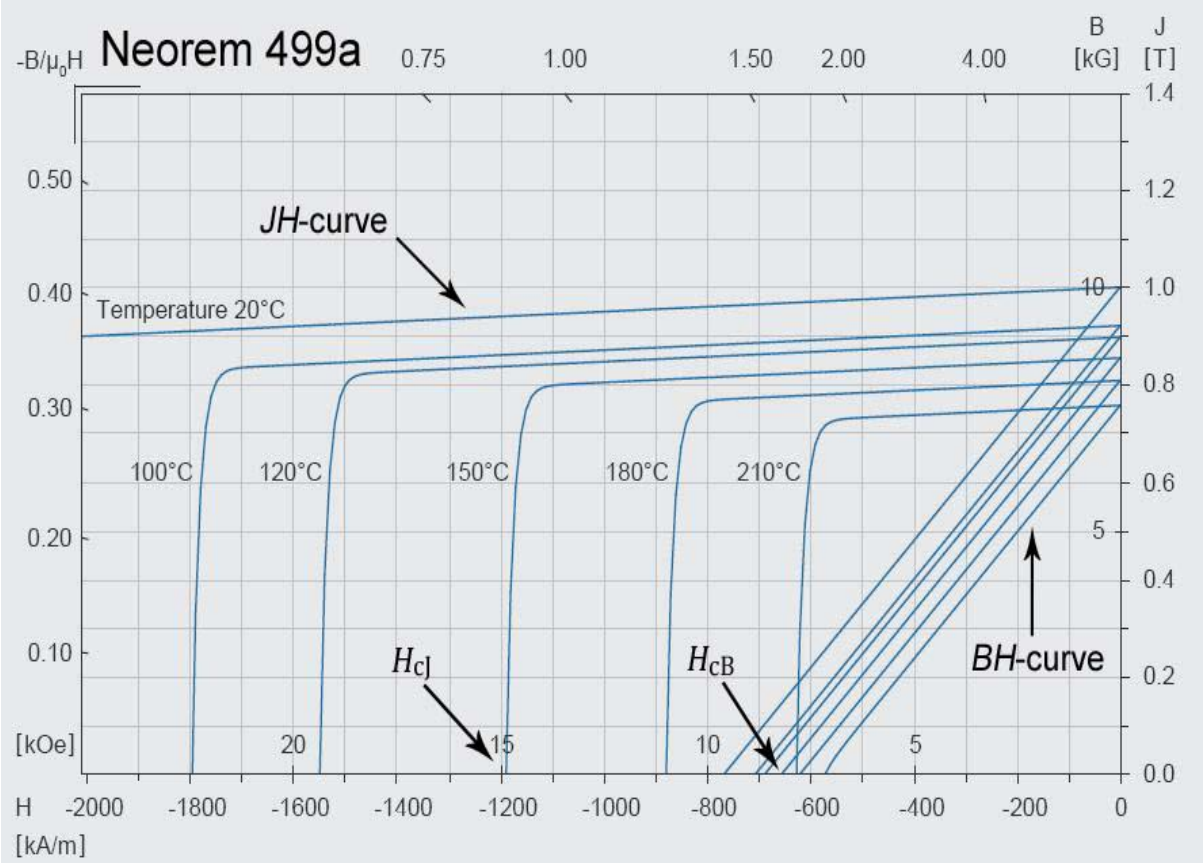

Figure 3 Second quadrant of the hysteresis curve of a NdFeB magnet material. (Neorem Magnets, 2011)

The examples at *JH*-curve and *BH* curves are shown in figure 3. Both of the curves have their crossing points which are marked in the figure. Usually, only the second quadrant curves of the hysteresis loops are shown. The vertical axis on the right side of figure 3 tells the value for the remanence B_r. There are shown different curves at different temperatures.

With such permanent magnet materials as the NdFeB and the SmCo, the power and the torque density of PMSM can be increased significantly. The machine designer should notice that the machine's thermal design is made carefully because the remanence of the permanent magnets will decrease when the temperature increases. Therefore, the heat transfer is important.

2.3 PM machine's rotor topologies

There are many kinds of different rotor topologies that can be used in the PM-machines. Figure 4 illustrates seven different PM rotor topologies.

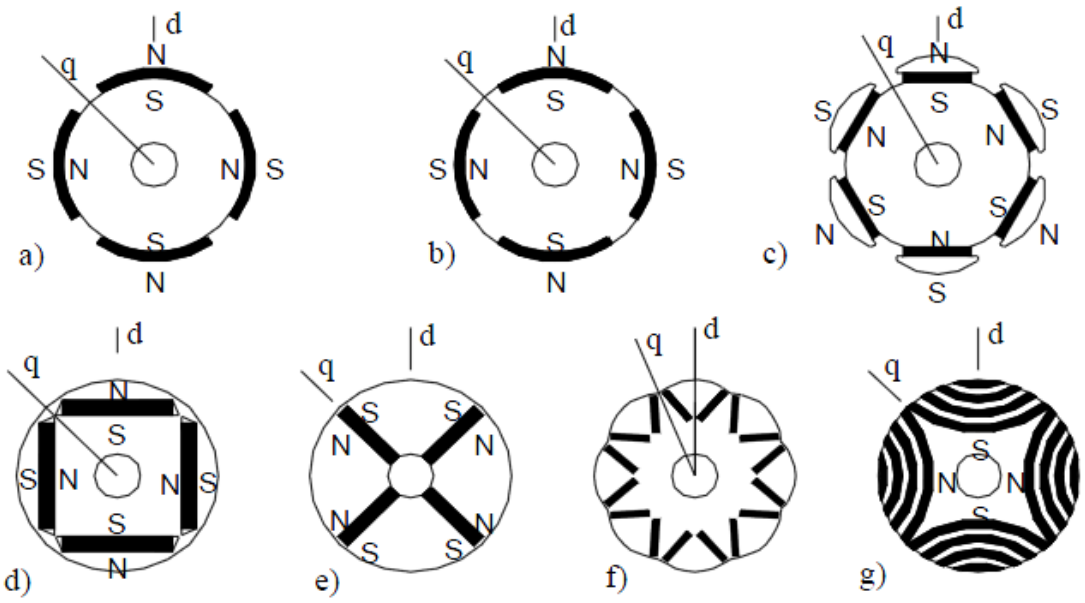

Figure 4 Rotor constructions of PM motors. (a) surface magnet rotor, (b) magnets embedded in the surface, (c) pole-shoe rotor, (d) single-barrier rotor, (e) radially embedded magnets, (f) V-magnet rotor, (g) synchronous reluctance rotor equipped with permanent magnets (Pyrhönen 2008, 397)

The rotor surface magnet PMSM (figure 4a) is non-salient and there is no significant inductance difference between the d- and q-axes as said earlier. This construction corresponds to a non-salient-pole electrically excited synchronous machine with fixed rotor current because the effective air gap of the machine is, in practice, constant irrespective of the observation position.

Other rotor types which are introduced in figure 4 can have some reluctance torque which is caused by the rotor saliency. Figure 4b illustrates magnets embedded in the rotor. That kind of construction has always inductance difference and normally the q-axis inductance is higher than the d-axis inductance. This is sometimes called inverse saliency because in salient pole synchronous machines the ratio of inductances is vice versa. This kind of rotor construction is well suited for the NdFeB magnets because a high level fundamental component of the air gap flux can be realized better with the high field magnet material and the magnet material is now less needed (Schiferl and Lipo 1990, 115).

The pole-shoe construction (figure 4c) has iron poles between the magnet segments. That kind of a rotor construction produces similar inductance ratio as a rotor with embedded magnets. The single-barrier design (figure 4d) gives acceptable field weakening perfor-

mance and if more barriers are added the saliency ratio and the reluctance torque proportion will increase.

The rotor construction with radially embedded magnets (figure 4e) has also good abilities in the field weakening applications but it tends to have relatively low reluctance torque (Soong(a) et al. 2007). That kind of construction requires flux barriers near the axis to prevent the flux from flowing through the axis (Pyrhönen 2009). The construction is mechanically challenging. A V-shaped magnet (figure 4f) construction is widely used in the traction applications and it can give a good inductance ratio. The V-type rotor constructions seem to be preferred in the hybrid electric vehicles and these V-type rotors are most used when the need of the reluctance torque is necessary for high speed operation in the field weakening region (Lindh et al. 2011).

The synchronous reluctance rotor (figure 4g) can be improved by adding permanent magnets in the rotor. Also the rotor types in figure 4d and figure 4e can operate like the synchronous reluctance machines without magnets. When the magnets are added the characteristics of the machine can be significantly improved when compared with the characteristics of regular synchronous reluctance machine. The efficiency and the power factor are better than the original synchronous reluctance machine.

The interior magnets have also some other advantages than rotor saliency. With the embedded magnets it is easier to vary the air gap flux density and the no-load flux density can also be made higher than with surface magnet rotors (Lindh et al. 2011). Also the magnets are mechanically safe when they are embedded inside the rotor and the demagnetization risk is also smaller than with the rotor surface-mounted magnets. This is because usually the machine with embedded magnets offers demagnetizing flux paths not travelling through the magnets themselves.

2.4 Torque and power equations for the PM machine

The following equations are for the interior PM machine. As said earlier the machine with embedded magnets produces torque with the magnets themselves and with the rotor saliency. The torque production can be calculated accordingly to cross-field principle

$$T = \frac{3}{2} p(\boldsymbol{\psi_s} \times \boldsymbol{i_s}), \tag{2.1}$$

where T is torque, p is a number of pole pairs, $\boldsymbol{\psi_s}$ is stator flux linkage vector and $\boldsymbol{i_s}$ is the stator current vector.

In the PM-machines the torque equation can be written in form

$$T = \frac{3}{2}p(\psi_{\mathrm{PM}} i_{\mathrm{sq}} + i_{\mathrm{sd}} L_{\mathrm{md}} i_{\mathrm{sq}} - i_{\mathrm{sq}} L_{\mathrm{mq}} i_{\mathrm{sd}}), \tag{2.2}$$

where ψ_{PM} is the flux linkage caused by the permanent magnets in the stator windings, i_{sq} is the q-axis stator current in the rotor reference frame, i_{sd} is the d-axis stator current in the rotor reference frame, L_{md} and L_{mq} are the magnetizing inductances of d- and q-axis.

The permanent magnet produces torque only with the q-axis current and the reluctance torque is generated by the terms $L_{\mathrm{mq}} i_{\mathrm{sq}}$ and $L_{\mathrm{md}} i_{\mathrm{sd}}$ and corresponding perpendicular currents i_{sd} and i_{sq}. The equation shows that the bigger the inductance difference is the bigger the reluctance torque will be.

With the permanent magnet machines the per unit (pu) values of magnetizing inductances differ significantly from the per unit values of for example traditional induction machines. A stator leakage is usually 0.1 pu (values are explained in App I) and in traction applications the d- and q-axes inductances are usually below 1 pu. It is usual that the quadrate axis synchronous inductance is larger than the direct axis synchronous inductance.

A load angle equation is also an important subject of the analysis in the case of the PM machine. The load angle equation with the RMS values can be written as

$$P = 3\left(\frac{U_{\mathrm{s}} E_{\mathrm{PM}}}{\omega_{\mathrm{s}} L_{\mathrm{d}}} \sin\delta + U_{\mathrm{s}}^2 \frac{L_{\mathrm{d}} - L_{\mathrm{q}}}{2\omega_{\mathrm{s}} L_{\mathrm{d}} L_{\mathrm{q}}} \sin 2\delta\right), \tag{2.3}$$

where ω_{s} is the electrical angular frequency of the stator flux, E_{PM} the permanent magnet flux linkage induced back electromotive force (EMF), U_{s} the supply voltage, L_{d} the direct axis synchronous inductance, L_{q} the quadrature axis synchronous inductance and δ the load angle.

Correspondingly can be written for the torque

$$T = \frac{mp}{\omega_{\mathrm{s}}^2}\left(\frac{U_{\mathrm{s}} E_{\mathrm{PM}}}{L_{\mathrm{d}}} sin\delta + U_{\mathrm{s}}^2 \frac{L_{\mathrm{d}} - L_{\mathrm{q}}}{2L_{\mathrm{d}} L_{\mathrm{q}}} sin2\delta\right), \tag{2.4}$$

where m is the number of phases. Equation (2.4) simplifies when the rotor surface magnet PM machine is in question. Then the latter term of the equation can be neglected because

there is no saliency and therefore no inductance difference either. The power equation (2.3) simplifies too, for the same reason.

The largest torque can be achieved in the PMSM with load angle that is well above 90 degrees. This is due to the reluctance difference because the q-axis inductance is often higher than d-axis inductance. This is demonstrated in figure 5.

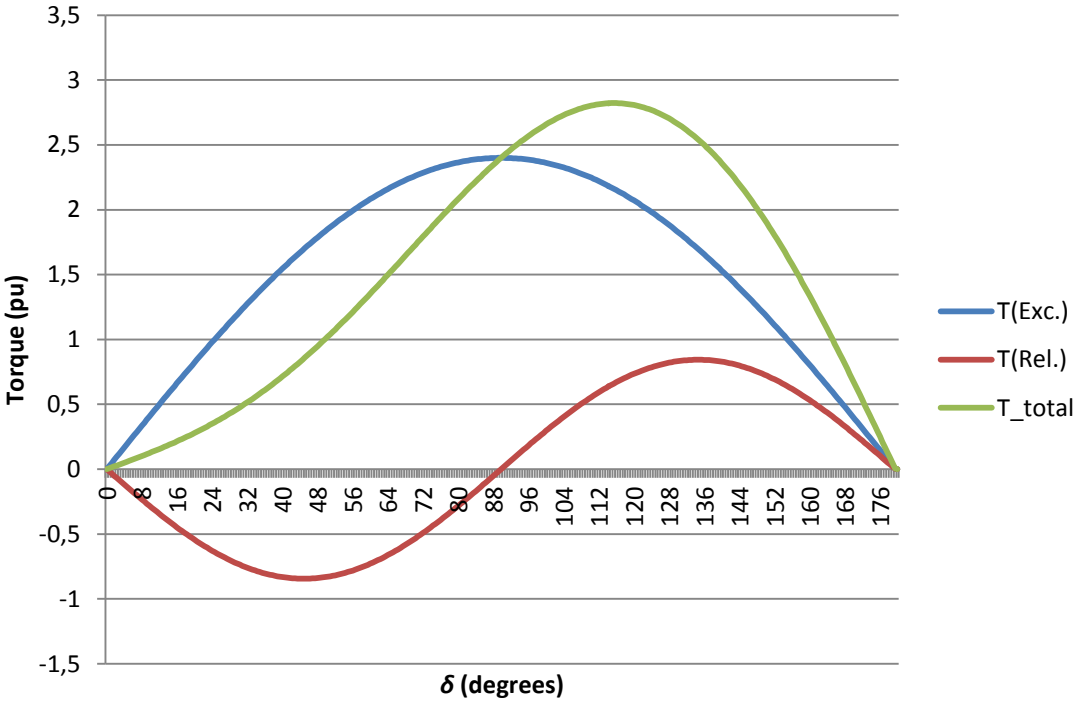

Figure 5 The torque as a function of the load angle δ for a PMSM with inverse saliency. E_{PM} = 0.8 pu, U_s = 0.9 pu, L_d = 0.3 pu and L_q = 0.8 pu

Figure 5 shows the torque as the function of the load angle for the SynRaPMSM with machine parameters E_{PM} = 0.8 pu, U_s = 0.9 pu, L_d = 0.3 pu and L_q = 0.8 pu. The excitation and the reluctance parts of the torque are shown separately and the calculations are done with equation (2.4). The total torque is also calculated and it can be seen that the torque is largest when the load angle is above 90 degrees as mentioned earlier.

2.5 Space-vector theory

There is a need to introduce the fundamentals of space-vector theory before introducing the two-axis model of PMSM equivalent circuit (Pyrhönen 2009). The main reason about why using the space-vector theory is that traditional single-phase equivalent circuit is not applicable to transient states even though it can be well used with the sinusoidal quantities. So the space-vector theory creates the solution for the problem of transients.

Following simplifying assumptions are used in the space-vector theory

1. the flux density distribution is sinusoidal in the air gap
2. the saturation of the magnetizing inductance is constant
3. there are no iron losses
4. the resistances and inductances are independent of the temperature and the frequency

The following equations show how the space-vector theory is mathematically defined. In the three-phase machine there is local 120 electrical degrees phase shift between the phases of the machine and because of that phase shift we have to introduce a phase-shift operator

$$\boldsymbol{a} = e^{j\frac{2\pi}{3}}. \tag{2.5}$$

In handling of the electrical machines necessary current, voltage and flux linkage space-vectors can be written in following equations

$$\boldsymbol{i_s}(t) = \frac{2}{3}[\boldsymbol{a}^0 i_{\mathrm{sA}}(t) + \boldsymbol{a}^1 i_{\mathrm{sB}}(t) + \boldsymbol{a}^2 i_{\mathrm{sC}}(t)], \tag{2.6}$$

$$\boldsymbol{u_s}(t) = \frac{2}{3}[\boldsymbol{a}^0 u_{\mathrm{sA}}(t) + \boldsymbol{a}^1 u_{\mathrm{sB}}(t) + \boldsymbol{a}^2 u_{\mathrm{sC}}(t)], \tag{2.7}$$

$$\boldsymbol{\psi_s}(t) = \frac{2}{3}[\boldsymbol{a}^0 \psi_{\mathrm{sA}}(t) + \boldsymbol{a}^1 \psi_{\mathrm{sB}}(t) + \boldsymbol{a}^2 \psi_{\mathrm{sC}}(t)], \tag{2.8}$$

where i_{sN}, u_{sN} and ψ_{sN} are the current, voltage and flux linkage of the phase N. The factor 2/3 reduces the length of the vector to the same value as the real amplitude of the sinusoidal corresponding variable and after reduction the parameters of the real equivalent circuit can be used in the calculations.

This space-vector theory helps to model the machine because with the space-vectors and coordinate transformations. When modelling the machine in practice we need to divide vectors in real- and imaginary parts. A model like this is known as the two-axis model. In many cases there are many advantages in changing the reference frames because in the rotor reference frame for example d- and q-axis inductances are constant. In the stator reference frame the inductances are not constant. Therefore, the transformation is usually done. Often in the vector control there is a big need to make coordinate transformations.

Therefore, the main reason of the space-vector theory is to help in the calculating and modelling of the machine.

The simplest representation for the coordinate transformation is achieved by using polar complex representation. In the stator coordinate system the rotating current can be written

$$i_s = ie^{j(\gamma+\theta)}. \tag{2.9}$$

When we want to change the coordination system we only need to be turned to required direction. The coordinate transformation is shown in figure 6.

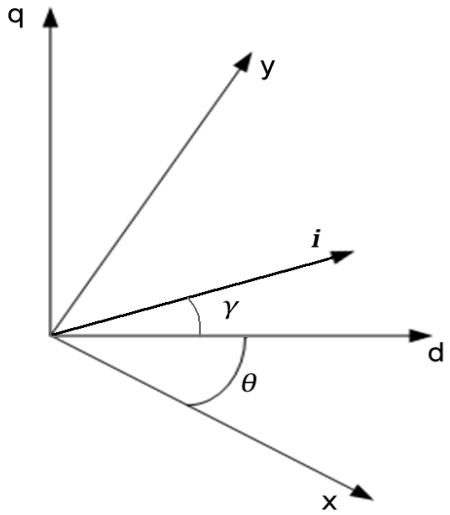

Figure 6 The current vector $\boldsymbol{i}$ in different reference frames. *xy* reference frame is the stator reference frame and *dq* is the rotor reference frame. θ is the rotor angle in stator reference frame and γ the current angle.

Figure 6 shows that for positive direction the change of the reference frame is done by multiplying at term $e^{j\theta}$ and for negative direction by multiplying at term $e^{-j\theta}$.

The stator voltage equation in the stator reference frame can be written as

$$\boldsymbol{u}_s^s = R_s \boldsymbol{i}_s^s + \frac{d\boldsymbol{\psi}_s^s}{dt}. \tag{2.10}$$

As the previous figure shows by multiplying by $e^{-j\theta}$, one gets the stator voltage equation in the rotor reference frame

$$\boldsymbol{u}_s^s e^{-j\theta} = \boldsymbol{u}_s^r = R_s \boldsymbol{i}_s^r + \frac{d\boldsymbol{\psi}_s^r}{dt} + j\omega_r \boldsymbol{\psi}_{s.}^r \tag{2.11}$$

This transformation of the reference frames is used in chapter 2.6 when the machine is modelled with the two-axis model in the rotor reference frame.

2.6 Equivalent circuit of PM machine

In common case all the synchronous machines are asymmetrical when examined from the stator point of view. Hence, we examine the synchronous machines in the rotor coordinate reference frame. Let us introduce next the equivalent circuit of the PM machine. Figure 7 shows the equivalent circuit of the PMSM corresponding to the two-axis model in the rotor reference frame. The effect of the damper windings has been neglected because in traction applications the damper windings are not used and the analysis simplifies.

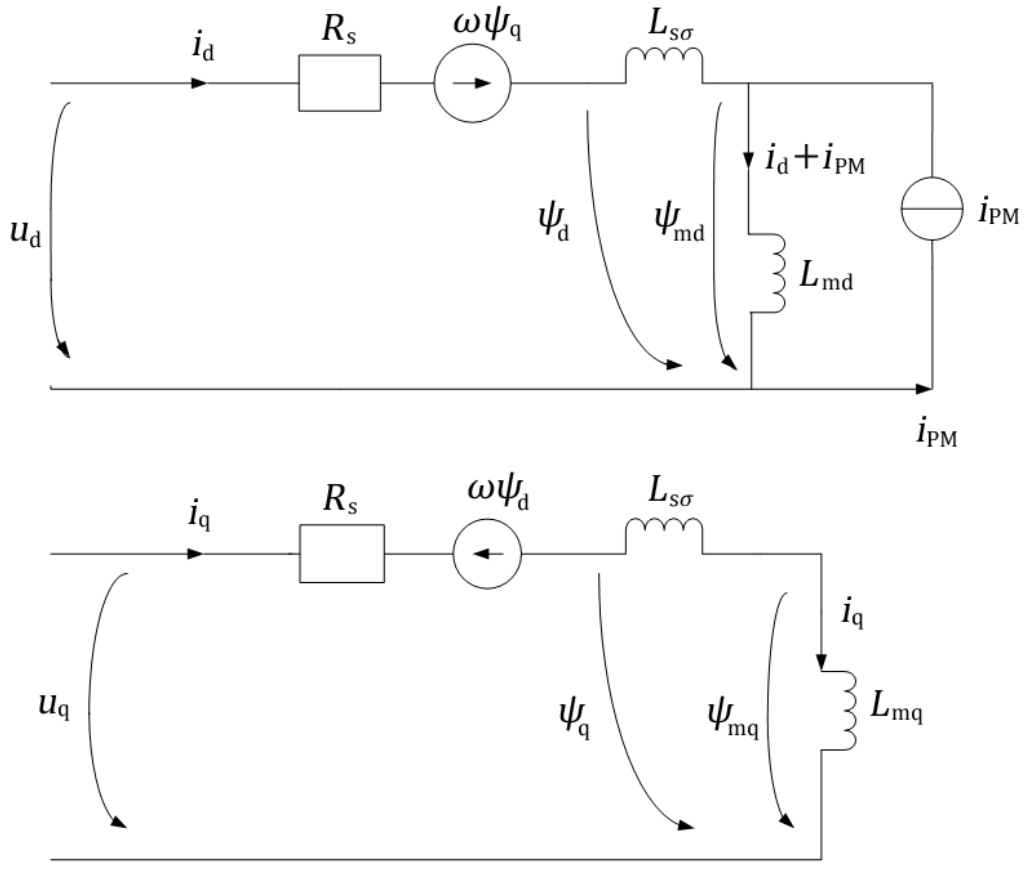

Figure 7 Equivalent circuits of PMSM in the d- and q-directions corresponding to the two-axis model in rotor reference frame. u_d is d-axis voltage, u_q q-axis voltage, ψ_d d-axis flux linkage, ψ_q q-axis flux linkage, ψ_{mq} q-axis air gap flux linkage, ψ_{md} d-axis air gap flux linkage, ω angular frequency, R_s stator resistance, $L_{s\sigma}$ stator leakage inductance, i_{PM} current source which describes the effect of permanent magnet.

The equations to the equivalent circuit parameters can be written by looking the previously presented equivalent circuit. Those parameters are all needed in defining the field weakening point of the synchronous reluctance permanent magnet machine. Let us specify these equations of the equivalent circuit parameters without the damper windings because for them is usually no use in traction applications. This results from the fact that in a traction application there nowadays always is an inverter which makes it possible to start the machine directly to the synchronous speed. The voltage equations can be written in the rotor reference frame:

$$u_{\mathrm{sd}} = R_{\mathrm{s}} i_{\mathrm{sd}} + \frac{d\psi_{\mathrm{sd}}}{dt} - \omega\psi_{\mathrm{sq}}, \tag{2.12}$$

$$u_{\mathrm{sq}} = R_{\mathrm{s}} i_{\mathrm{sq}} + \frac{d\psi_{\mathrm{sq}}}{dt} + \omega\psi_{\mathrm{sd}}. \tag{2.13}$$

Often it is enough to examine the machine when it is in a steady state. During this work the machine is also examined in steady state, and the previous voltage equations can be written then as

$$u_{\mathrm{sd}} = R_{\mathrm{s}} i_{\mathrm{sd}} - \omega\psi_{\mathrm{sq}}, \tag{2.14}$$

$$u_{\mathrm{sq}} = R_{\mathrm{s}} i_{\mathrm{sq}} + \omega\psi_{\mathrm{sd}}. \tag{2.15}$$

The resultant voltage of these voltage d- and q-axis components can be written in form

$$u = \sqrt{u_{\mathrm{sd}}^2 + u_{\mathrm{sq}}^2}. \tag{2.16}$$

The stator flux linkage components in the equations (2.14) and (2.15) are determined by the equations

$$\psi_{\mathrm{sd}} = L_{\mathrm{sd}} i_{\mathrm{sd}} + \psi_{\mathrm{PM}}, \tag{2.17}$$

$$\psi_{\mathrm{sq}} = L_{\mathrm{sq}} i_{\mathrm{sq}}. \tag{2.18}$$

The synchronous inductances consist of the magnetizing inductance and the leakage inductance $L_{\mathrm{s}\sigma}$. The equations of synchronous inductances can be written in form

$$L_{\mathrm{sd}} = L_{\mathrm{md}} + L_{\mathrm{s}\sigma}, \tag{2.19}$$

$$L_{\mathrm{sq}} = L_{\mathrm{mq}} + L_{\mathrm{s}\sigma}. \tag{2.20}$$

Inserting (2.19) and (2.20) into equations (2.17) and (2.18), it can be written for the flux linkage components

$$\psi_{\mathrm{sd}} = (L_{\mathrm{md}} + L_{\mathrm{s}\sigma})i_{\mathrm{sd}} + \psi_{\mathrm{PM}}, \tag{2.21}$$

$$\psi_{\mathrm{sq}} = (L_{\mathrm{mq}} + L_{\mathrm{s}\sigma})i_{\mathrm{sq}}. \tag{2.22}$$

The air gap flux linkages can be written in form

$$\psi_{\mathrm{md}} = L_{\mathrm{md}}i_{\mathrm{d}} + \psi_{\mathrm{PM}}, \tag{2.23}$$

$$\psi_{\mathrm{mq}} = L_{\mathrm{mq}}i_{\mathrm{q}}. \tag{2.24}$$

Equations (2.21) and (2.23) show that only the stator leakage components differ the air gap flux linkage components from the stator flux linkage components. As the previous equations showed the effect of the permanent magnet material affects only in the d-axis. The stator voltage in d- and q axis can now be written with equations (2.21) and (2.22) into the form

$$u_{\mathrm{sd}} = R_{\mathrm{s}}i_{\mathrm{sd}} - \omega(L_{\mathrm{mq}} + L_{\mathrm{s}\sigma})i_{\mathrm{sq}}, \tag{2.25}$$

$$u_{\mathrm{sq}} = R_{\mathrm{s}}i_{\mathrm{sq}} + \omega(L_{\mathrm{md}} + L_{\mathrm{s}\sigma})i_{\mathrm{sd}} + \omega\psi_{\mathrm{PM}}. \tag{2.26}$$

The total stator flux linkage can be calculated with the previous flux linkage components like the voltage before

$$\psi_{\mathrm{s}} = \sqrt{\psi_{\mathrm{sd}}^2 + \psi_{\mathrm{sq}}^2}. \tag{2.27}$$

The air gap flux can be calculated in the same way

$$\psi_{\mathrm{m}} = \sqrt{\psi_{\mathrm{md}}^2 + \psi_{\mathrm{mq}}^2}. \tag{2.28}$$

The flux linkage ψ_{PM} which is created by the permanent magnet can be written by an equivalent field current

$$i_{\mathrm{PM}} = \frac{\psi_{\mathrm{PM}}}{L_{\mathrm{md}}}. \tag{2.29}$$

The field current i_{PM} is not constant because of the saturation of the magnetizing inductance L_{md}. The saturation is very difficult to model. Modelling is studied later on this thesis.

The power factor of the machine can be written in form

$$\cos\varphi = \frac{u_{sd}i_{sd}+u_{sq}i_{sq}}{ui}. \tag{2.30}$$

The equations above are used to calculate all equivalent circuit parameters for the SynRaPMSM.

2.7 Vector diagram of the PMSM

All previous equations can be proven also with the vector diagram of the permanent magnet synchronous machine. The vector diagram is very important in defining the operating state of the machine. The vector diagram of the PMSM, when it works in the motor mode, is shown in the figure 8. The motor works close to its base speed.

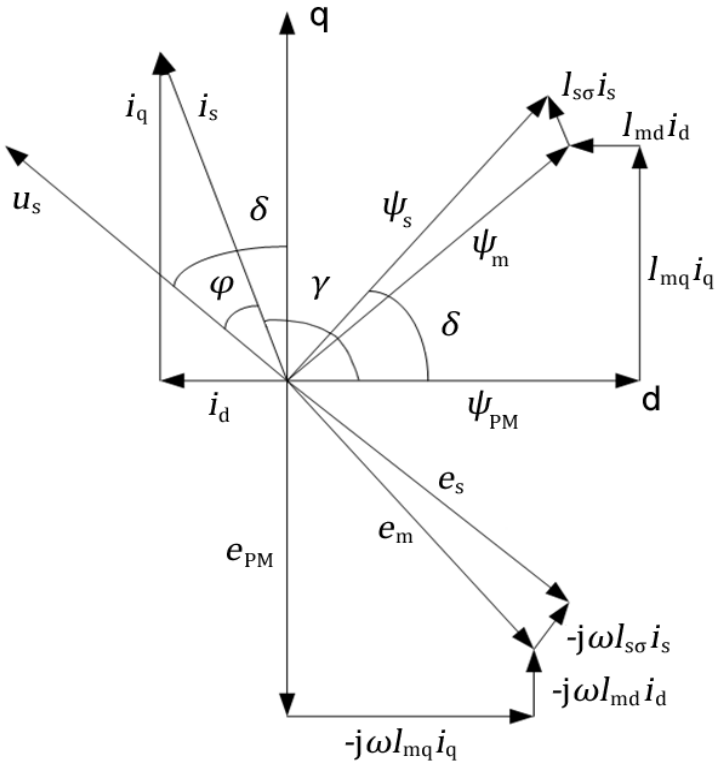

Figure 8 Vector diagram of the PMSM close to the base speed.

Figure 8 shows the vector diagram according to the motor logic speed, ω = 0.9 pu. Other parameters in per unit values are: ψ_{PM} = 0,75 pu, i_q = 0,75 pu, i_d = -0,3 pu, l_{mq} = 0,66 pu,

l_{md} = 0,5 pu , $l_{s\sigma}$ = 0,1 pu. Current i_s is 0.8 pu and voltage u_s is 0.72 pu. Now the stator flux linkage ψ_s can be calculated in per unit values by using equations (2.21), (2.22) and (2.27) and 0.8 pu is obtained. The torque can be calculated now from equation (2.2). The value for the torque output of this machine is 0.6 pu. The stator resistance is neglected. Remarkable is that a negative d-axis current is used which means that the PM flux is reduced. The machine is working now close to its base speed.

The basics of the per unit value calculation are presented in the appendix 1 and per unit values are used later on this thesis.

2.8 Current angle based equations

For the controlling of the stator current it is clearer to use the current angle γ instead of the load angle δ. The vector control uses the current angle as a parameter and the direct torque control (DTC) uses the load angle. This thesis is done with such an assumption that the machine is controlled with the vector control. The same calculation can be utilized also with DTC but then one must use the load angle. Both of the control methods are studied shortly in the end of the chapter 3. Figure 9 shows the vector diagram that takes into account the stator resistance.

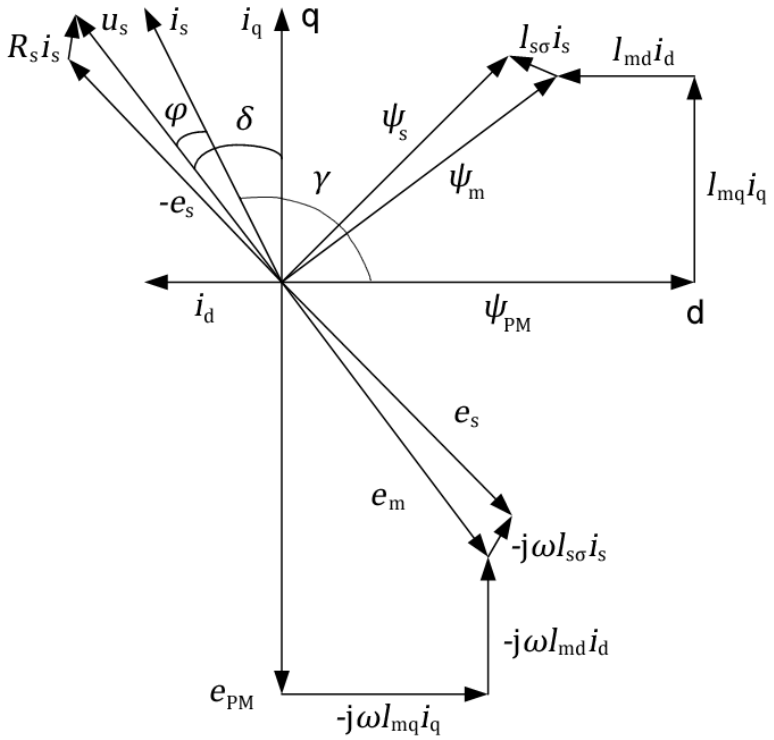

Figure 9 Vector diagram to make clear equations for the current angle γ as parameter. That vector diagram is used for per unit calculations.

In figure 9 it can be seen that the current angle γ is the angle between the stator current resultant i_s and d-axis current component i_d. Next equations are defined from the vector diagram. The power equation can be written with power factor $\cos\varphi$ into the form

$$P = 3u_{\mathrm{sph}} i_{\mathrm{s}} \cos\varphi \tag{2.31}$$

By looking the vector diagram it can be seen that the electrical power

$$P = 3u_{\mathrm{sph}} i_{\mathrm{s}} \cos\left(\left(\frac{\pi}{2} - \delta\right) - \gamma\right). \tag{2.32}$$

By remembering that

$$\cos\left(\frac{\pi}{2} - \delta\right) = \sin\delta, \tag{2.33}$$

we get the power into the form

$$P = 3u_{\mathrm{sph}} i_{\mathrm{s}} \sin(\delta - \gamma). \tag{2.34}$$

The power can be modified more

$$P = 3u_{\mathrm{sph}} i_{\mathrm{s}} \sin\delta \cos\gamma + 3u_{\mathrm{sph}} i_{\mathrm{s}} \cos\delta \sin\gamma. \tag{2.35}$$

Let us define the equations for the current components next

$$i_{\mathrm{d}} = i_{\mathrm{s}} \cos\gamma, \tag{2.36}$$

$$i_{\mathrm{q}} = i_{\mathrm{s}} \sin\gamma. \tag{2.37}$$

For the voltage components can be written

$$u_{\mathrm{d}} = u_{\mathrm{s}} \cos\delta = \psi_{\mathrm{PM}} + L_{\mathrm{d}} i_{\mathrm{d}}, \tag{2.38}$$

$$u_{\mathrm{q}} = u_{\mathrm{s}} \sin\delta = L_{\mathrm{q}} i_{\mathrm{q}}. \tag{2.39}$$

The output power of the motor can be written with equations (2.36), (2.37), (2.38) and (2.39) as

$$P = \Omega \left(i_s \psi_{PM} \sin\gamma - \left(\frac{L_q - L_d}{2} \right) i_s^2 \sin(2\gamma) \right). \quad (2.40)$$

For the torque it can be written

$$T = \frac{P}{\Omega} = \frac{3}{2} p(\psi_{PM} i_q + (L_d - L_q) i_d i_q). \quad (2.41)$$

The stator voltage in terminals is directly proportional to the rotational speed of the machine for a given stator current magnitude and the current angle. Hence the voltage constraint becomes more important when the machine's speed is high. The term characteristic current, which is studied in many papers, for example (Soong (a) et al. 2007), (Soong (b) et al. 2007), should be defined here

$$I_x = \frac{\psi_{PM}}{L_d} = i_d. \quad (2.42)$$

The characteristic current is an important parameter for the controlling of the machine as will be shown later on this thesis.

The action in the machine operations is limited by the voltage and current constraints when the stator current i_s and the stator voltage u_s is limited as follows

$$i_s = \sqrt{i_d^2 + i_q^2} \leq i_{s,max}, \quad (2.43)$$

$$u_s = \sqrt{u_d^2 + u_q^2} \leq u_{s,max} = \frac{U_{DC}}{\sqrt{3}}. \quad (2.44)$$

where $i_{s,max}$ is decided by the continuous stator current rating and the available output current of the inverter. The voltage limit $u_{s,max}$ is decided by the available maximum output voltage U_{DC} of the inverter.

To make those constraints clear just to remind that the voltage is shown as an ellipse and current is shown as a circle. The permitted operation zone of the machine is presented in figure 10.

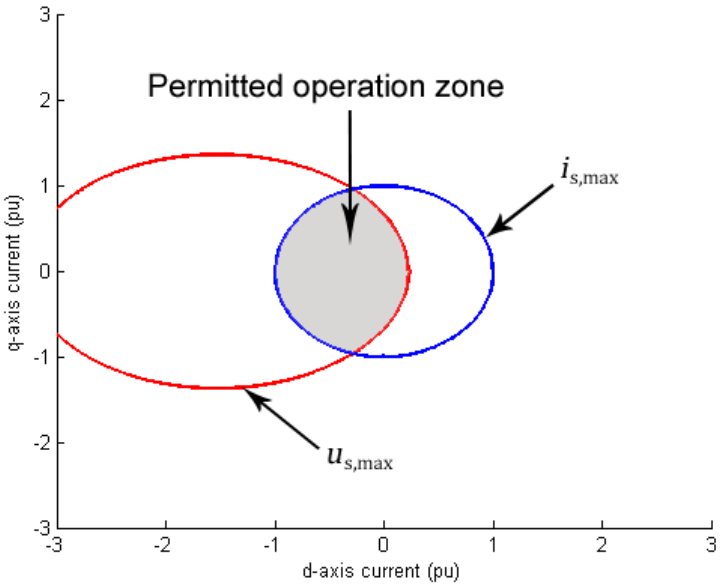

Figure 10 Permitted operation zone of the machine when the current and voltage constraints are determined. Parameters of the machine are L_d = 0.4 pu, L_q = 0.66 pu, ψ_PM = 0.62 pu.

In figure 10 it can be seen that the permitted operation zone is dependent on both of the current and the voltage. Those limitations should be in use at the same time. This makes the control and operation of the machine challenging at higher speeds because the voltage ellipse gets smaller when the speed is increased. It means that then the flux will decrease.

And for clarification, in per unit calculation

$$\omega_\mathrm{pu} = \frac{\omega}{\omega_\mathrm{n}} = \frac{n}{f_\mathrm{n}} = n_\mathrm{pu}. \tag{2.45}$$

Equation (2.45) shows that in per unit calculation the angular frequency and the speed are the same. That is why the terms are used mixed later in this thesis.

Now the total stator voltage can be written with equations (2.25) and (2.26) to the form

$$u_\mathrm{s}^2 = (R_\mathrm{s} i_\mathrm{sd} - \omega L_\mathrm{q} i_\mathrm{sq})^2 + (R_\mathrm{s} i_\mathrm{sq} + \omega L_\mathrm{d} i_\mathrm{sd} + \omega \psi_\mathrm{PM})^2. \tag{2.46}$$

By using the equations of the current components (2.36) and (2.37), the equation (2.46) can be written

$$u_\mathrm{s} = \sqrt{(R_\mathrm{s} i_\mathrm{s} \cos\gamma - \omega L_\mathrm{q} i_\mathrm{s} \sin\gamma)^2 + (R_\mathrm{s} i_\mathrm{s} \sin\gamma + \omega L_\mathrm{d} i_\mathrm{s} \cos\gamma + \omega \psi_\mathrm{PM})^2}. \tag{2.47}$$

Now one can see the effect of the armature reaction in the d-axis. The inductance L_{d} tries clearly to reduce the flux of the d-axis. The controlling of the machine is presented in the next chapter.

3. CONTROL METHODS OF PM-MACHINE

There is a need to introduce the control methods of the PM machine before one can understand its properties in the field weakening. One must be aware which control method is used and, especially, when the certain control method is used. The functional constraints must be defined. When one has the machine with an inverter one must always be conscious of by which control method the machine has been driven.

3.1 i_d = 0 – control

This control method is used with machines in which the permanent magnets are placed on the rotor surface. In the rotor surface magnet machines there is no significant inductance difference. Now the torque equation (2.2) is getting simpler.

$$T = \frac{3}{2} p \psi_{\mathrm{PM}} i_{\mathrm{sq}}. \tag{3.1}$$

Equation (3.1) is the torque equation for rotor surface magnet synchronous machines which do not have a significant asymmetry in the iron parts of rotor and consequently do not have any remarkably inductance difference. If one use ferrites in the rotor surface magnet machine, then some inductance difference is achieved. Now, the direct axis current does not have any effect on the torque and only the q-axis current i_{sq} produces torque. One can see that the only thing that has impact on torque is the stator current. This control method is poor when the machine has significant stator inductance because the amplitude of the stator flux linkage increases as a function of the torque

$$|\psi_{\mathrm{s}}| = \sqrt{\psi_{\mathrm{PM}}^2 + (\frac{TL_{\mathrm{sq}}}{\frac{3}{2}p\psi})^2}. \tag{3.2}$$

The problem with i_{d} = 0 – control is that the field weakening is not possible unless d-axis current does not have negative reference when the i_{d} = 0-principle is no more valid, at all. It can be seen in the name of this control method that the field weakening is not available at all. This control method is probably the easiest one when the field weakening is not needed.

3.2 Maximum torque per ampere – control (MTPA)

Next let us consider the maximum torque per ampere (MTPA) –control method which is also called the method for minimizing the stator current. The aim of this method is that for a given torque demand, the current amplitude is minimized to get the maximum torque with minimum current. The minimum point for the stator current at a constant torque is ob-

tained by finding the minimum distance of the hyperbola from the origin. Let us repeat the torque equation (2.41) here

$$T = \frac{3}{2}p\left(\psi_{\mathrm{PM}} i_{\mathrm{sq}} - L_{\mathrm{q}} i_{\mathrm{sd}} i_{\mathrm{sq}} + L_{\mathrm{d}} i_{\mathrm{sd}} i_{\mathrm{sq}}\right). \tag{3.3}$$

Here we see that the reluctance torque component has significance only with significant inductance difference. The torque equation can be modified with equations (2.36) and (2.37) into the form

$$T = \frac{3}{2}p(\psi_{\mathrm{PM}} I_{\mathrm{s}} \sin\gamma - \frac{(L_{\mathrm{q}} - L_{\mathrm{d}})}{2} I_{\mathrm{s}}^2 \sin 2\gamma). \tag{3.4}$$

where γ is the current vector angle in the rotor reference frame. The task is now to find the minimum value for the ratio of the torque and stator current as a function of γ. To obtain a fast transient response and a high torque, the current angle γ must be controlled to develop the maximum torque. That relationship between the stator current and the current angle can be derived by calculating the derivative of torque equation and setting the derivative with respect to current angle to zero. The derivative is

$$\frac{dT}{d\gamma} = -\frac{3}{2}p\psi_{\mathrm{PM}} I_{\mathrm{s}} \cos\gamma + \frac{3}{2}p\left(L_{\mathrm{q}} - L_{\mathrm{d}}\right) I_{\mathrm{s}}^2 \cos 2\gamma = 0. \tag{3.5}$$

By remembering that

$$\cos 2\gamma = 2\cos^2\gamma - 1, \tag{3.6}$$

the optimal current angle γ can be solved from the equation (3.5). The optimal direct-axis current when the determined γ is substituted can now be written in the form

$$i_{\mathrm{d\_MTPA}} = \frac{\psi_{\mathrm{PM}} - \sqrt{{\psi_{\mathrm{PM}}}^2 + 8(L_{\mathrm{q}} - L_{\mathrm{d}})^2 |i_{\mathrm{s}}|^2}}{4(L_{\mathrm{q}} - L_{\mathrm{d}})}. \tag{3.7}$$

The optimal quadrature-axis current can be written

$$i_{\mathrm{q\_MTPA}} = \sqrt{{i_{\mathrm{s}}}^2 - {i_{\mathrm{sd}}}^2}. \tag{3.8}$$

The current references are obtained at previous equations (3.7) and (3.8) if the speed controller is in use. This control method is also very poor in the field weakening applica-

tions because the curve form of the current is distorted away from the sine form and the torque contains lots of ripple. This leads to the problem that currents cannot be minimized. Use of d-axis demagnetizing current is now compulsory to decrease the flux. So the MTPA goes easily to the field weakening but the control method changes in the field weakening area and when the voltage limit is reached then the field weakening of the machine really starts and the MTPA is no more useful control method (Pyrhönen 2009).

3.3 Field weakening – control

When the MTPA-control strategy is not in use, the field weakening (FW)-control takes place. Now the aim is to control the d-axis current in that way that it will demagnetize the PMSM and weaken the stator flux. The torque reduces when this control method is in use. The equations for the current components can be calculated by defining them under the voltage constraint (Haque et al. 2003).The equations of the current components in the field weakening can be calculated by equations

$$i_{\mathrm{d\_FW}} = \frac{L_{\mathrm{d}}\psi_{\mathrm{PM}} - \sqrt{(L_{\mathrm{d}}\psi_{\mathrm{PM}})^2 + \left(L_{\mathrm{q}}^2 - L_{\mathrm{d}}^2\right)\left(\psi_{\mathrm{PM}}^2 + L_{\mathrm{q}}^2 i_{\mathrm{s}}^2 - u_{\mathrm{s}}^2/\omega^2\right)}}{L_{\mathrm{q}}^2 - L_{\mathrm{d}}^2}, \tag{3.9}$$

$$i_{\mathrm{q\_FW}} = \sqrt{i_{\mathrm{s}}^2 - i_{\mathrm{d\_FW}}^2}. \tag{3.10}$$

All these parameters, which are shown in the previous two equations, are the rated values of the machine. When the speed is increasing the voltage is inversely proportional to the rotating speed of the machine and the new values for the current components can be calculated with two previous equations in every point, when the field weakening control method is used to control the stator flux. Figure 11 demonstrates the principles of the previously presented MTPA- and FW-control strategy.

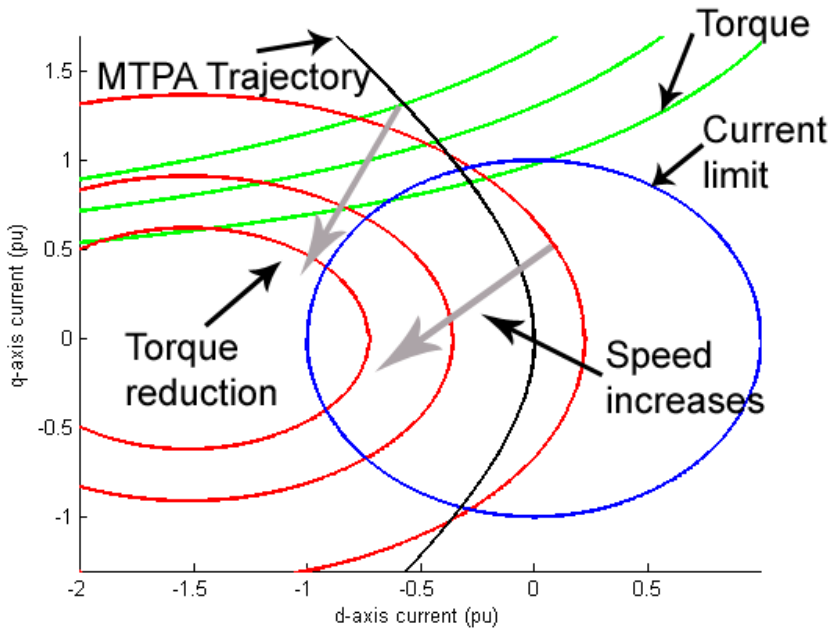

Figure 11 Principles of field weakening control strategy. Parameters of the machine are L_d = 0.4 pu, L_q = 0.66 pu, ψ_{PM} = 0.62 pu.

It is shown in figure 11 that the torque is reduced in the field weakening range. The green lines in the figure are constant torque trajectories. The black line is the MTPA-trajectory which gives the maximum torque at certain current. It is shown that if the speed is increasing the limitations gets stricter and for that condition the magnitude of demagnetizing current should increase to fulfil torque demands. The centre point of the ellipses is given by the characteristic current I_x of the motor. I_q is always zero at the centre point of the voltage ellipses.

When the nominal rotational speed is achieved the control method changes from MTPA to the FW-control. Then the torque is reduced and the current angle γ is controlled so that the magnitude of the stator current is in its nominal value. And then the control is towards end the FW-control or in some special situations more power can be achieved by changing the control method to maximum torque per volt.

3.4 Maximum torque per volt -control (MTPV)

In the case of limited voltage operation the armature current must be controlled. The target of this method is that for a given torque demand, the voltage is limited. This condition occurs when the characteristic current of the machine is smaller than 1. Taking the first derivative of the torque equation with respect to $\mathrm{d}T/\mathrm{d}i_d$ and using equation (3.9), the armature current vector producing the maximum amount of the output torque under the volt-

age constraint can be derived (Illioudis and Margaris 2010). The equations which can be used in controlling the armature current can be written as follows

$$i_{\mathrm{d\_MTPV}} = -\frac{\psi_{\mathrm{PM}}}{L_{\mathrm{d}}} - \Delta i_{\mathrm{d}}, \tag{3.11}$$

$$i_{\mathrm{q\_MTPV}} = \frac{\sqrt{(\frac{U_{\mathrm{S}}}{\omega})^2 - (L_{\mathrm{d}}\Delta i_{\mathrm{d}})^2}}{L_{\mathrm{q}}}, \tag{3.12}$$

where

$$\Delta i_{\mathrm{d}} = \frac{-\frac{L_{\mathrm{q}}}{L_{\mathrm{d}}}\psi_{\mathrm{PM}} + \sqrt{(\frac{L_{\mathrm{q}}}{L_{\mathrm{d}}}\psi_{\mathrm{PM}})^2 + 8\left[\left(\frac{L_{\mathrm{q}}}{L_{\mathrm{d}}} - 1\right)\left(\frac{U_{\mathrm{S}}}{\omega}\right)\right]^2}}{L_{\mathrm{q}}}. \tag{3.13}$$

The equations are qualified only in the MTPV-control. The MTPV-control is used when the use of the MTPA- and the field weakening control methods are not valid. MTPV-control can approve the torque and power in the end of machine operations but can only be used when the characteristic current is smaller than one. In the case where the characteristic current is bigger than one MTPV-curve is not considered because it lies then outside the current limit circle.

In MTPV-region the current is always

$$i_{\mathrm{s\_MTPV}} < i_{\mathrm{s,max}}, \tag{3.14}$$

and that is why the MTPV-control occurs only when the MTPV-curve lies inside the current circle. MTPV-control operation is always done with the voltage which is equal to the voltage limit.

3.5 Control mode selection

As previous analysis is shown the MTPA and current limit trajectories are independent of the speed of the machine. These trajectories are only determined by the motor parameters. The voltage limit trajectory varies with the machine's speed. The voltage ellipse contracts when the speed increases (Haque et al. 2002). Theoretically the motor can have the infinite speed if voltage ellipse is only a point inside the current limit circle (Schiferl and Lipo 1990).

Figure 12 shows the analysis of the control mode selection between the MTPA mode, the field weakening mode and the MTPV control.

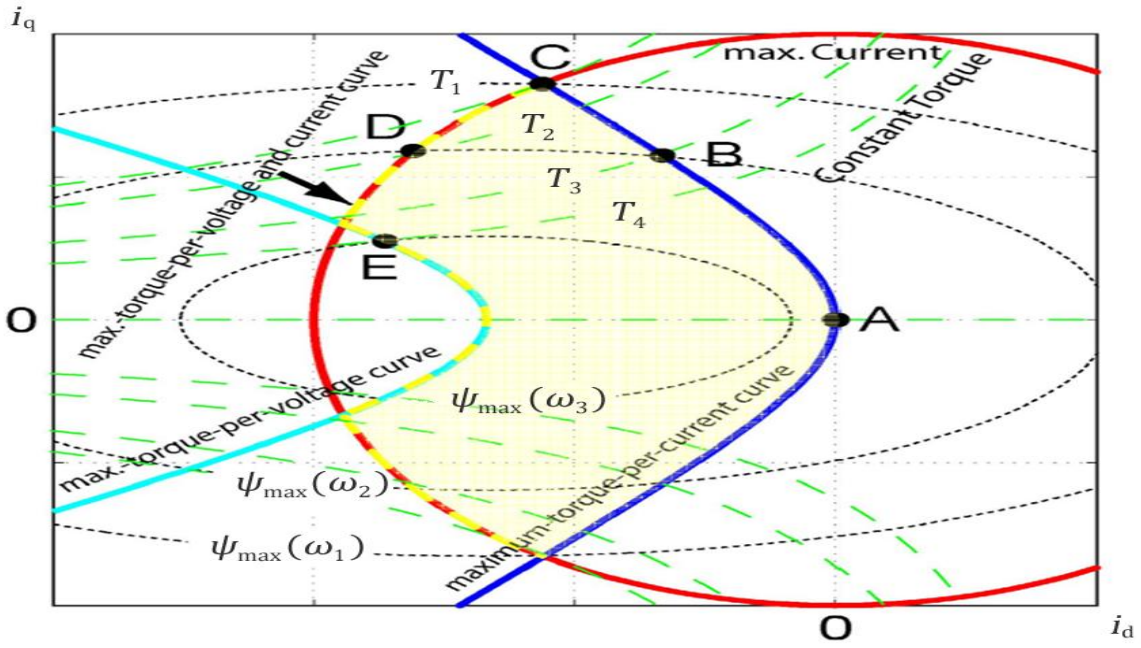

Figure 12 Trajectories of the control of the PMSM (Meyer et al. 2007).

In figure 12 it can be seen the area where the machine should operate at any condition. The red circle is the maximum current circle. The dotted green lines are the constant torque trajectories, the blue line shows us the line of the MTPA- control method and the light blue curve is the MTPV curve. The dotted black lines show the voltage per the speed ellipses or shortly the flux linkage ellipses. The light yellow area between all those curves and lines is the permitted operation zone of the machine.

It can be seen from the previous figure which control strategy is used at different conditions. During low speeds the operations of the machine can be controlled by the MTPA and then one can choose the point on the MTPA line. The maximum amount of torque can be generated in the point C. In the point C, the motor has the rated current and the rated voltage and will produce the rated torque at base speed. Further than the point C, cannot be achieved because of the current limit. The control mode selection between the MTPA and the field weakening control must be done in point C. Whether the MTPA or field weakening should be selected is determined by the motor speed and the load.

For higher rotor speeds the use of the field weakening control strategy is compulsory and if the operation point moves along the current circle, when the maximum available torque is achieved, more and more negative d-axis current is needed to reach that torque. If the desired torque is the line T_3 the operating is moved to the voltage limit. After that, if the

operation point E is wanted to be achieved, and the voltage ellipse condition are fulfilled, then the MTPV-control is used. The characteristic current is smaller than 1 pu when MTPV is in use.

3.5.1 Vector control

The same principles are used in the vector control of the PMSM as ordinary synchronous machines. The vector control is implemented in the rotor reference frame, in which the control creates current references i_{dref} and i_{qref} for the direct axis and quadrature axis components and implements these references by tuning the voltage value. Usually these current references are created directly of the torque reference but there is also other method. A rotation speed controller can be used to define currents by the stator current reference i_{sref}. When the d- and q-current references are formed, then the two-phase-to-three-phase transformation is done. The coordinate transformation is done by the methods that were studied earlier.

The current vector control is widely used to control the permanent magnet synchronous machines. With the vector control the control properties are good and the efficiency of the permanent magnet drive is quite high. The principal block diagram of the vector control is implemented in figure 13.

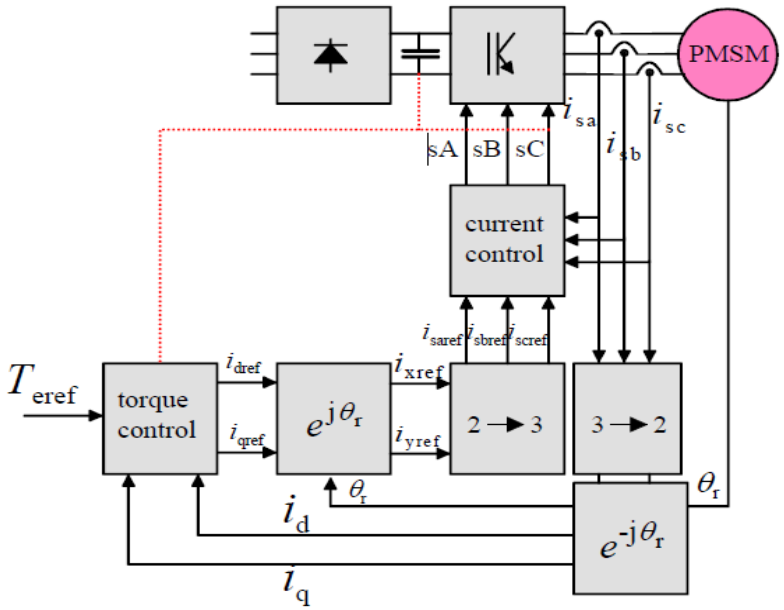

Figure 13 Block diagram of the current vector control of the PMSM (Pyrhönen 2009).

In figure 13 it can be seen that the rotor angle position θ is needed in the vector control of the permanent magnet machine. This block diagram illustrates to the torque control based vector control. First the change in the stator reference frame from three phase to two

phase presentation is done. Then with the rotor position information the d- and q-axis currents are formed in the rotor reference frame. The current references are created with the torque reference. The rotor angle position is needed again to move back in the stator reference frame. The two-phase-to-three-phase transformation is done and then the current references realized by a current controller. The inverter can feed the currents in the stator of the PMSM.

3.5.2 Direct torque control (DTC)

Let us introduce the direct torque control method next by a short preview even the current angle based vector control has been chosen for control method in this thesis. In current angle based vector control the current can be controlled directly. In DTC the current is an output variable resulting from the flux linkage control of the machine.

The Direct torque control (DTC) was first presented by Takahashi and Noguchi (1986) for the induction machines. DTC is useful control method also in the case of PMSM. DTC is based on the controlling of the flux linkage and the torque directly. There is no need to determine any reference currents in the DTC because the flux linkage can be estimated directly in the stator reference frame by the integral

$$\psi_{\mathrm{s,est}} = \int \left(u_{\mathrm{s,est}} - i_{\mathrm{s,meas}} R_{\mathrm{s}}\right) \mathrm{d}t, \tag{3.15}$$

where $u_{\mathrm{s,est}}$ is the stator voltage estimate, $i_{\mathrm{s,meas}}$ the measured current and $\psi_{\mathrm{s,est}}$ the stator flux linkage estimation.

Equation (3.15) shows that the calculation of the stator flux linkage is dependent only on the stator voltage estimate and the stator resistance and no other machine parameters are needed. Because of the direct flux control DTC suits well for operation in the constant-power range and probably it is consequently the best control method in traction applications.

The DTC has also some problems: the voltage is not measured directly but it is estimated from the DC intermediate voltage and the switch models. At low speeds the resistive voltage drop can become a dominating factor and so the flux linkage estimate can easily become erroneous (Pyrhönen 2009). The other problem with DTC is to determine the optimal flux linkage and torque with respect to the optimal efficiency, and when that is established, the efficiency must still be taken into account of current and voltage limitations.

Another stator flux linkage estimate in the machine is received by computing the stator flux linkage with the machine parameters (Takahashi & Nokuchi 1986). Then the information of the rotor angle is needed and with that information the so called current model can be used. The current model equations are shown in (3.16) and (3.17).

$$\psi_{\mathrm{sd}} = L_{\mathrm{sd}} i_{\mathrm{sd}} + L_{\mathrm{md}} i_{\mathrm{D}} + \psi_{\mathrm{PM}} \tag{3.16}$$

$$\psi_{\mathrm{sq}} = L_{\mathrm{sq}} i_{\mathrm{sq}} + L_{\mathrm{mq}} i_{\mathrm{Q}} \tag{3.17}$$

Usually in traction applications the damper parts $L_{\mathrm{md}} i_{\mathrm{D}}$ and $L_{\mathrm{mq}} i_{\mathrm{Q}}$ can be neglected. DTC needs the information of the load angle δ. If one wants to use the load angle based DTC instead of the current angle based vector control to control the machine, with the help of figure 9 vector diagram the equations for the power and the torque can be written. These equations are already presented in equations (2.3) and (2.4).

4. FIELD WEAKENING OF PM-MACHINE

One of the main tasks when designing an electrical machine in traction application is to know how the machine works in the field weakening. The field weakening is needed in a situation when the target is to make the motor rotate at a speed higher than the machine's rated speed. The field weakening can be reached by increasing the frequency. The voltage of the motor cannot be increased together with the rotational speed because the voltage has already reached its rated value. Now when the voltage is kept constant at its rated value and the frequency is increased, the U/f-ratio decreases and at the same time the flux linkage diminishes.

The field weakening creates a big problem with the PMSM because the permanent magnet creates its own fixed flux which cannot be controlled. Designing the motor for a wide constant-power region can be critical in presence of low inductance values. The only way to drive the PMSM deep into the field weakening is to use demagnetizing current i_d. The demagnetizing current creates often other problems. The stator Joule losses will increase due to the high negative i_d current. Another negative consequence is the risk of non-reversible demagnetization of permanent magnets, which may possibly never be capable of getting back their remanent flux density B_r (Luise et al. 2010).

In the field weakening area, some or even all the stator current is consumed in reducing the stator flux linkage. This means that more stator current is needed in the field weakening range than corresponding constant flux range.

When designing of a PMSM is started, it is extremely important to choose the flux linkage provided by the permanent magnets and the machine's inductances correctly. This kind of PMSM drive must always contain some voltage reserve, usually c. 10 % of the stator voltage.

The principles of the field weakening are presented in figure 14.

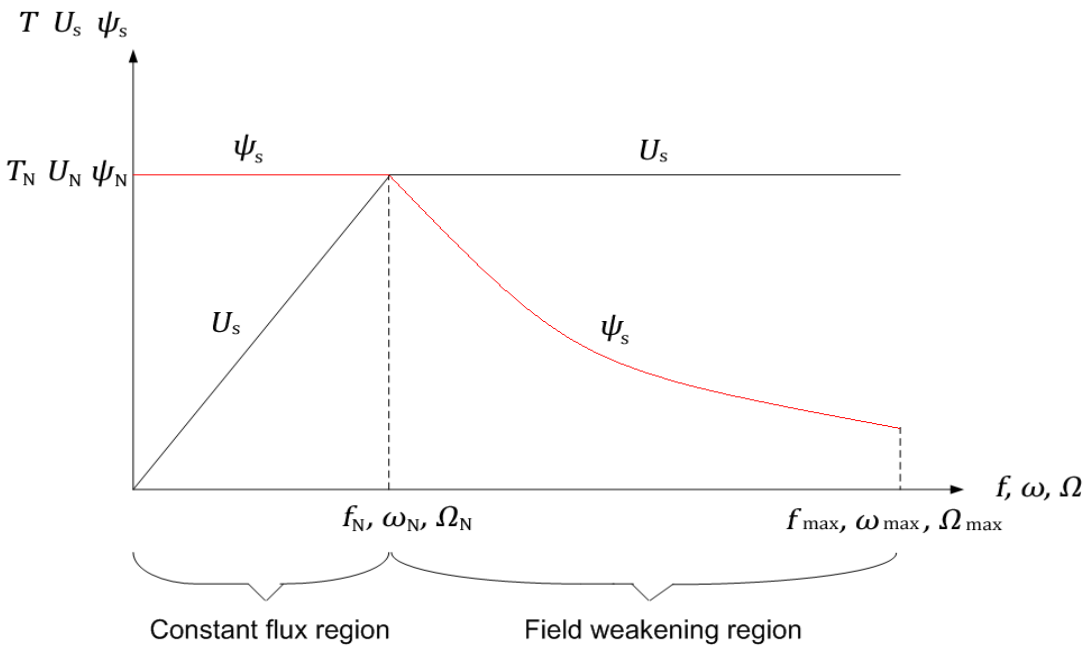

Figure 14 The principles of field weakening. Constant flux region and field weakening region are shown. Ω is mechanical angular speed, f_{max} maximum frequency, ω_{max} maximum electrical angular frequency, Ω_{max} maximum mechanical angular frequency.

In figure 14 it can be seen that the area where the field weakening really starts is very narrow. Below the rated speed the area is called the constant flux region. Now the voltage is increasing and the flux is kept constant. In that area the field can be controlled by using for example the MTPA-control method in order to have low losses and fast transient response. Also in the constant flux region the flux control should be used if the rotor core becomes saturated to produce torque (Chy and Uddin 2007). Also the other control methods can be used in the constant flux region.

The next area of the figure 14 is the field weakening region where the speed is above the rated speed. Now the voltage is kept constant and the flux is decreasing. Then it is not possible to get more torque than in the constant flux region due to the current and voltage constraints. To get to that region the use of demagnetizing d-axis current is compulsory. i_d = 0-control cannot be used anymore in the field weakening region. Then the FW-control takes its place.

In the field weakening area the control of the flux is very important. The d-axis current should be controlled in a manner that it will weaken the flux linkage by the armature reaction and the leakage flux linkage and the terminal voltage is constant all the time. The result of the weakening of the armature flux is that the total air gap flux is reduced.

One big task when using the permanent magnet synchronous machine in the field weakening is to remember that the back EMF caused by the permanent magnets is directly proportional to the rotational speed of the machine. This leads to the problem of endurance of the inverter because if the demagnetizing current is lost for some reason, the inverter should tolerate this voltage. Usually the inverter cannot endure this EMF but it is totally damaged (Pyrhönen 2009). However, in case of traction drives the converter DC-link is often parallel to a battery and in such a case the drive just brakes heavily when the battery is charged via the free-wheeling diodes of the inverter bridge. Of course the converter current capability may not be exceeded.

If one relies on the inverter's ability to operate deep in the field weakening, the motor can run faster than the maximum DC intermediate voltage limited speed. The maximum speed of the machine can be reached if the inverter's current reserve is totally in use.

The upper limit for the field weakening without the inverter's current limit can be determined according to the maximum DC link intermediate voltage

$$f_{\mathrm{fwp,lim}} = \frac{U_{\mathrm{DCmax}}}{E_{\mathrm{PM}} \cdot \sqrt{6}} \cdot f_{\mathrm{n}}, \tag{4.1}$$

where f_{n} is the rated frequency of the machine and U_{DCmax} the maximum DC link intermediate voltage. If the motor's rated current is used to demagnetize the machine, the speed range can be increased. And finally when the inverter's current reserve is fully used the speed range cannot be increased any more.

4.1 Machine losses and efficiency

Let us study the interior PM machine losses next. It is very important to discuss about the machine efficiency when the design of permanent magnet machine is started. In the machine the key types of losses are: iron, copper and magnet losses. Iron losses can be significant in interior PM machines when the machine is used in the field weakening range. High iron losses can make significant problems in the interior PM machines over wide constant-power ranges. Iron losses can be divided into

- Stator iron losses
- Rotor iron losses
- PWM switching iron losses

The stator losses are often increasing under field weakening conditions. The flux density harmonics co-operate with the direct axis armature reaction flux and produce high losses

in the stator yoke and the stator teeth even though the fundamental flux magnitude is decreased (Soong(a) et al. 2007).

The rotor losses are caused by the stator slot harmonics. The rotor iron losses create about 10 % of the total iron loss at the maximum speed for example in a single-barrier interior machine design. The PWM iron losses are significant usually at lower speeds and form about 15 % of the total iron losses at the maximum speed.

The biggest amount of the iron losses are formed in the stator. The iron losses can be minimized in many ways, for example, by increasing the stator slot openings, changing the angular positions of the rotor barriers and optimally designing the stator and rotor geometries (Soong(a) et al. 2007).

Among iron losses the other big source of losses are the copper losses. These losses are significant, especially, in interior PM machines. The copper losses are biggest when the machine is driven at high speed and when the machine is loaded light. Under these conditions the machine is fed with large demagnetizing d-axis current. The copper losses can be consisted by three different reasons. These reasons are

- Skin-effect
- Proximity effect
- Eddy currents

The previous effects can be reduced by using conductors which are bundles of multiple, thin insulated strands and ensuring appropriate transposition of both the conductors within each bundle, and of the bundle position within the slot.

The copper losses are known as Joule losses of the stator and can be derived from the equation

$$P_{\mathrm{J}} = 3R_{\mathrm{s}}I_s^2. \tag{4.2}$$

The interior permanent magnet machines do not suffer from the magnet losses much because the permanent magnet material is sheltered inside the rotor iron parts and hence the high frequency flux variations do not harm the magnets (Soong(a) et al. 2007).

On the other hand the surface permanent magnet machines share of losses is divided differently. The magnet losses are then in a major role because the magnets are mounted

on the surface of the rotor. In that kind of structure the magnets are not mechanically safe and the harmonics of the flux may harm the magnet material. The magnet losses are based on the eddy currents that are caused by the magnetic field variations produced by the armature reaction of the stator windings. Also a small contribution from the stator slotting forms the eddy current losses (Soong(a) et al 2007).

And finally of course every machine type have additional losses which shall never be forgotten when the losses are estimated.

4.2 Choosing a converter for the machine

One important task is choosing the right converter for the electrical machine drive. Power electronic devices have done the use of electrical machines a lot easier, more economical and – last but not least – more energy efficient. When the power electronic converter is matched to the motor and the load, a few things must be taken into account. The power electronic converter and its control depend on the motor type which is selected. The main circuit components of a two level voltage source power electronic converter are shown in figure 15.

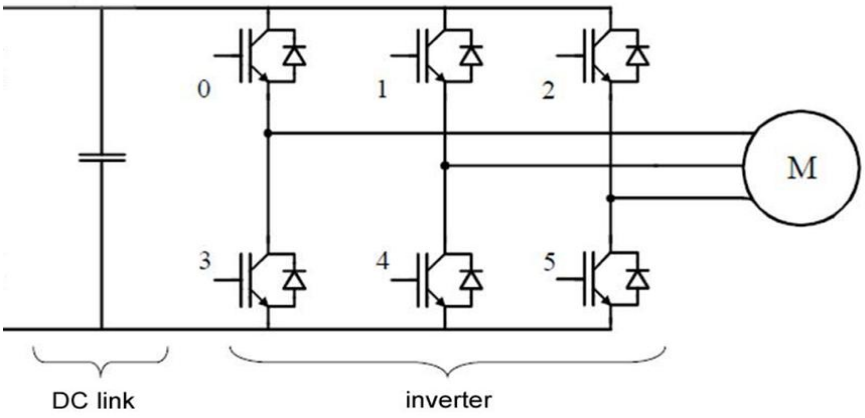

Figure 15 Converter drive main circuit components.

Figure 15 shows that the converter consists a DC link and an inverter. The DC link's function is to operate at energy storage and to reduce the distortion from the voltage. The DC voltage is inverted back to the AC voltage in inverter with the semiconductor switches. Now the voltage, which magnitude and frequency can be adjusted, can be fed to the motor.

The power electronic converter provides a controlled voltage to the motor for controlling the current of the machine and, hence, the electromagnetic torque of the motor. The fol-

lowing things listed here should always be defined when the converter is matched to the motor (Mohan et al. 2003, 372-373).

- Current rating
- Voltage rating
- Switching frequency
- Motor inductance
- Speed sensor or speed sensorless

The converter should tolerate a certain time the demanded current that corresponds to the maximum torque needed. The voltage should be greater than the counter back emf produced by the motor. The magnitude of the emf in a motor increases linearly with the motor speed and hence the voltage rating of the converter depends on the maximum motor speed with a constant air gap flux.

The steady state ripple in the motor current should be as small as possible to minimize the motor losses and the ripple of the torque. A small current ripple needs large inductances. The ripple in the current can be reduced also by increasing the switching frequency of the converter. The losses of the converter increase linearly with the switching frequency. Therefore, the selection of the inductances and the switching frequency is a compromise to be made.

The salient pole machine is more complicated to control than a rotor surface magnet machine. The advantage of the saliency is though at lower costs of the machines because less magnet material is needed (Schiferl and Lipo 1990, 117).

4.3 Saturation effect

The saturation effect of inductances must be taken into account when the machine is designed. The saturation has been analysed a lot at the moment and it differs in each machine. When the modelling of saturation is done, it is always only near to the right results. The modelling of saturation effect is very difficult and it needs many measurements before the equation of the saturation of the electric machine can be written. Saturation of the inductances is strongly dependent on the positions of the magnets in the rotor. In this chapter, some kind of an estimation for the cross coupling effect of the inductances is done.

In PMSM the d-axis saturation can be neglected because it is so small (Zhu et al. 2007) but the q-axis saturation should be taken in to account. The electromagnetic torque accounting for the influence of cross-coupling is given by (Zhu et al. 2009)

$$T = \frac{3}{2}p\left[\psi_{\mathrm{PM}}(i_{\mathrm{q}})i_{\mathrm{q}} + \left(L_{\mathrm{d}}(i_{\mathrm{d}}, i_{\mathrm{q}}) - L_{\mathrm{q}}(i_{\mathrm{d}}, i_{\mathrm{q}})\right)i_{\mathrm{d}}i_{\mathrm{q}}\right]. \tag{4.3}$$

When the saturation effect is taken into account the voltage can be represented with voltage d- and q-axis components

$$u_{\mathrm{s}} = \sqrt{(-\omega L_{\mathrm{q}}(i_{\mathrm{d}}, i_{\mathrm{q}})i_{\mathrm{q}} + R_{\mathrm{s}}i_{\mathrm{d}})^2 + (\omega\psi_{\mathrm{PM}}(i_{\mathrm{q}}) + \omega L_{\mathrm{d}}(i_{\mathrm{d}}, i_{\mathrm{q}})i_{\mathrm{d}} + R_{\mathrm{s}}i_{\mathrm{q}})^2}. \tag{4.4}$$

Figure 16 illustrates the effect of cross saturation for the d-axis inductance in the interior PMSM.

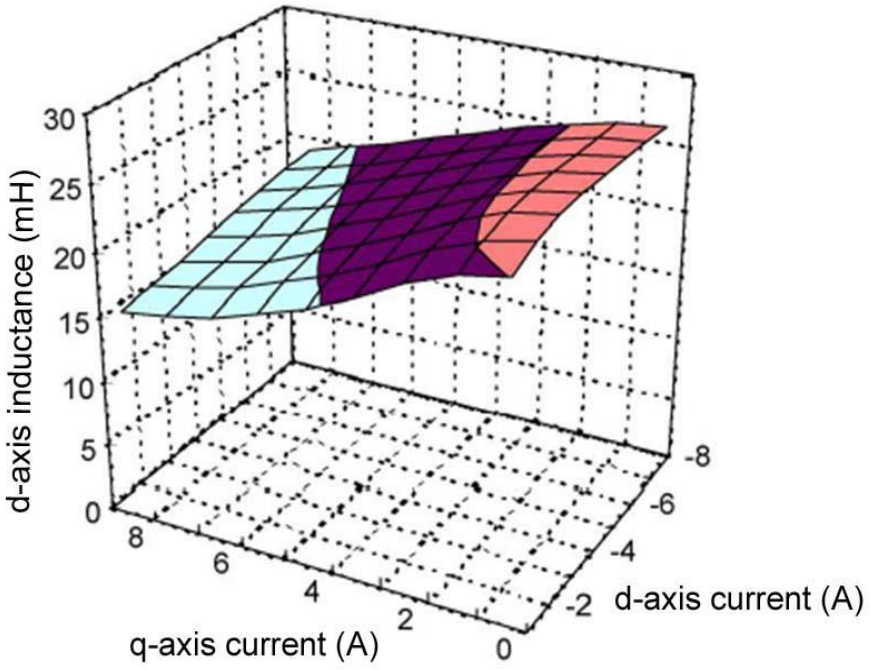

Figure 16 d-axis inductance accounting for cross coupling in the interior PMSM (Zhu et al. 2009).

Figure 16 shows the saturation effect of the d- axis inductance. The direct axis magnetizing inductance is presented as a function of quadrature axis current i_{q} and the direct axis current i_{d}. The d-axis inductance increases little with an increase of the d-axis current and it reduces significantly with an increase of the current i_{q}. In figure 17 it is shown the effect of cross coupling in the q-axis inductance.

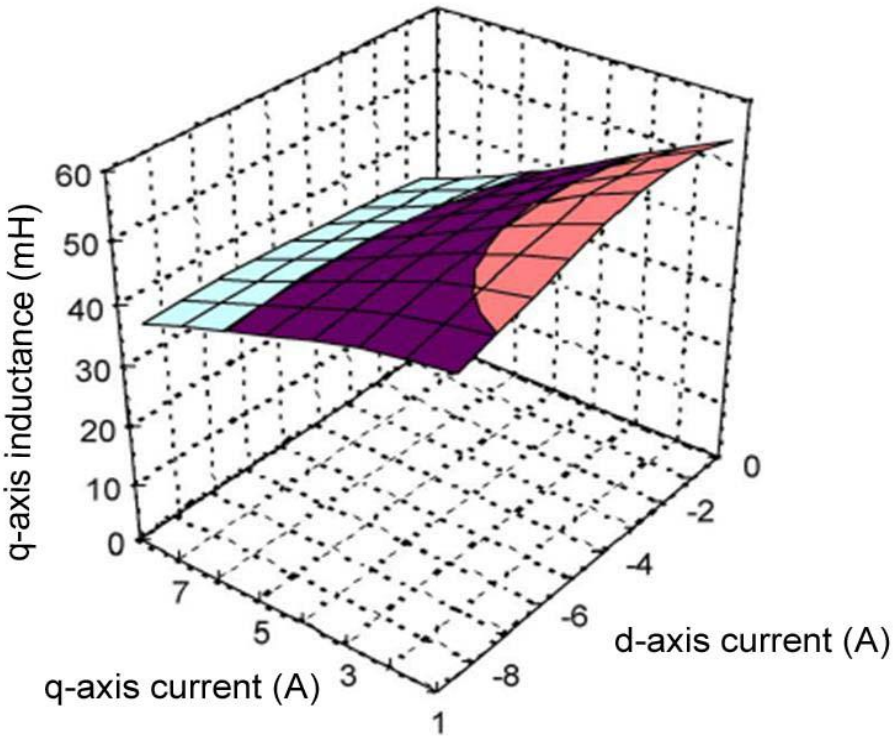

Figure 17 q-axis inductance accounting for cross coupling in the interior PMSM (Zhu et al. 2009).

Figure 17 shows the saturation effect of the q-axis inductance. In the figure it can be seen that the q-axis inductance L_{q} reduces strongly when the q-axis current is increased. When the current i_{q} is large then the inductance L_{q} changes very little according to the current i_{d}. The variation of the flux linkage caused by the permanent magnets with q-axis current is shown in figure 18.

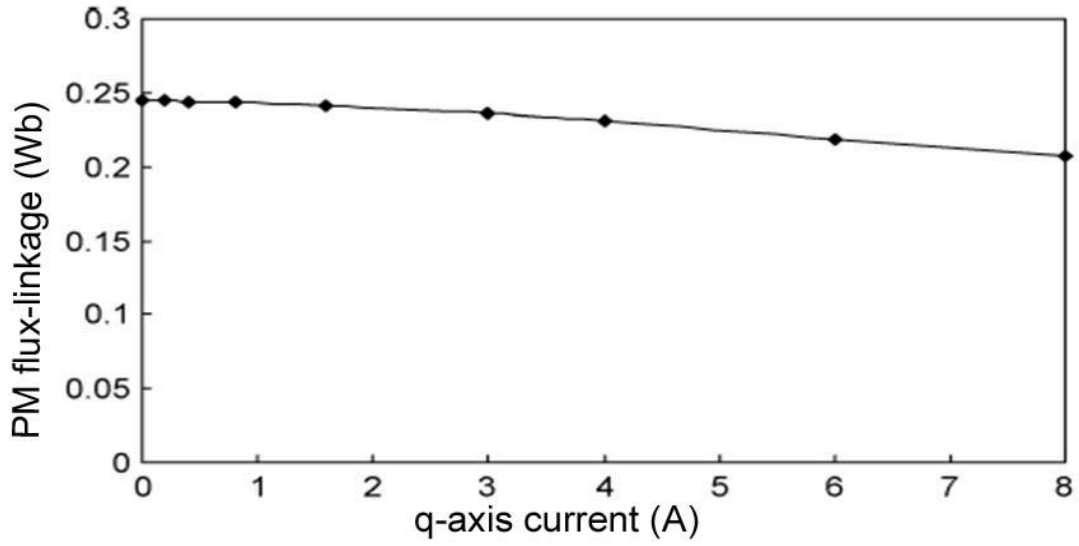

Figure 18 The variation of the flux linkage ψ_{PM} with q-axis current (Zhu et al. 2009).

In figure 18 it can be seen that ψ_{PM} reduces when the q-axis current is increasing. This corresponds to the loss of polarization in the magnet under the influence of the demagnetizing field strength in Fig. 3. So the saturation effect will affect the flux linkage caused by the PM, too. In practice the current i_{d} will affect to ψ_{PM} also but it will be now assumed that the effect of i_{d} can be neglected because that effect is relatively small.

Now when the machine's cross saturation is presented in figures 16 and 17, and the assumption is made that the cross saturation of traction PMSM is close to the previous presentation, and there is a need to prepare models for the inductances. It can be written that

$$L_{\mathrm{d}}(i_{\mathrm{d}}, i_{\mathrm{q}}) = \frac{\psi_{\mathrm{d}}(i_{\mathrm{d}}, i_{\mathrm{q}}) - \psi_{\mathrm{PM}}(i_{\mathrm{q}})}{i_{\mathrm{d}}}, \tag{4.5}$$

$$L_{\mathrm{q}}(i_{\mathrm{d}}, i_{\mathrm{q}}) = \frac{\psi_{\mathrm{q}}(i_{\mathrm{d}}, i_{\mathrm{q}})}{i_{\mathrm{q}}}, \tag{4.6}$$

$$\psi_{\mathrm{PM}}(i_{\mathrm{q}}) = \psi_{\mathrm{d}}(i_{\mathrm{d}} = 0, i_{\mathrm{q}}). \tag{4.7}$$

The basic reason for cross saturation effect is the armature reaction of the stator windings which is due to the reluctance difference of the synchronous reluctance assisted permanent magnet machines. It should be noted that the above three equations for L_{d}, L_{q} and ψ_{PM} are only approximate. Next the models must be made.

4.3.1 Saturation models for the magnetizing inductances

The model for the saturation of the inductances is done by assuming the torque-speed characteristics of the interior PMSM with stator slot-pitch skew. Skew is accounted for by dividing the length of the machine into several slices, analysing each slide independently and then combining results. Of course, the positions of the d- and q-axis of each slice relative to the current will differ. Figure 19 shows the relative positions of the d- and q axes in unskewed and skewed machines. So the skewing effects to the size of the current angle.

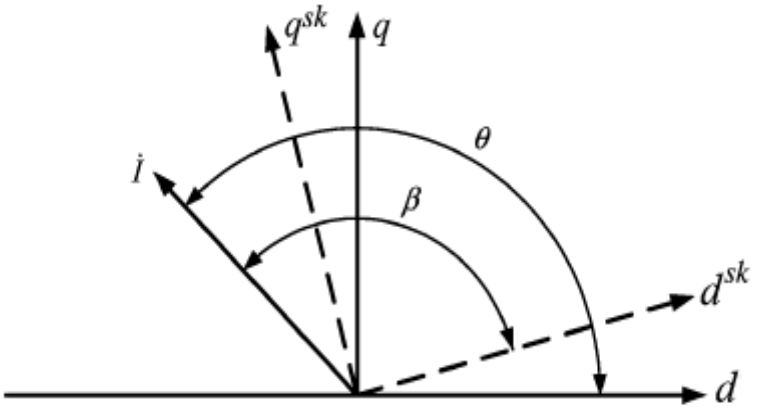

Figure 19 Positions of d- and q-axis in unskewed and skewed machines. θ and β are the current phase angles relative to the d-axis of the skewed and unskewed machines (Zhu et al 2009).

By looking at figure 19 the saturation models for the d- and q-axis inductances can be done (Zhu et al. 2009). Models are taking into account the cross coupling effect which was already examined in the previous chapter. Now the d- and q-axes of a skewed machine are assumed to be coincident with those of an unskewed machine at the centre of the machine. So the d- and q-axis flux linkages produced by the armature reaction in the skewed machine can be obtained

$$\psi_{\mathrm{d}}^{\mathrm{sk}} = \frac{1}{\alpha}\int_{\theta-\alpha/2}^{\theta+\alpha/2}\left[L_{\mathrm{d}}\left(i_{\mathrm{d}}, i_{\mathrm{q}}\right) i_{\mathrm{d}} \cos(\theta-\beta) - L_{\mathrm{q}}\left(i_{\mathrm{d}}, i_{\mathrm{q}}\right) i_{\mathrm{q}} \sin(\theta-\beta)\right]\mathrm{d}\beta, \tag{4.8}$$

$$\psi_{\mathrm{q}}^{\mathrm{sk}} = \frac{1}{\alpha}\int_{\theta-\alpha/2}^{\theta+\alpha/2}\left[L_{\mathrm{d}}\left(i_{\mathrm{d}}, i_{\mathrm{q}}\right) i_{\mathrm{d}} \cos(\theta-\beta) + L_{\mathrm{q}}\left(i_{\mathrm{d}}, i_{\mathrm{q}}\right) i_{\mathrm{q}} \sin(\theta-\beta)\right]\mathrm{d}\beta. \tag{4.9}$$

After integration the equations for the inductances can be written

$$L_{\mathrm{d}}^{\mathrm{sk}} = \frac{\psi_{\mathrm{d}}^{\mathrm{sk}}}{I_{\mathrm{n}}\cos\theta} = L_{\mathrm{d}}^{\mathrm{sk}} + \frac{1-K_{\mathrm{sk}}}{2}(L_{\mathrm{q}} - L_{\mathrm{d}}), \tag{4.10}$$

$$L_{\mathrm{d}}^{\mathrm{sk}} = \frac{\psi_{\mathrm{q}}^{\mathrm{sk}}}{I_{\mathrm{n}}\sin\theta} = L_{\mathrm{q}}^{\mathrm{sk}} - \frac{1-K_{\mathrm{sk}}}{2}(L_{\mathrm{q}} - L_{\mathrm{d}}). \tag{4.11}$$

where the superscript sk means the machine with skew and inductances without the superscript are derived directly from figures 16 and 17. The current I_{n} is the nominal current of the machine. K_{sk} is the skewing factor and it can be written

$$K_{\mathrm{sk}} = \frac{\sin\alpha}{\alpha}, \tag{4.12}$$

where α is the electrical skew angle. The i_q and i_d currents are assumed to be constants in calculating the inductances by equations (4.10) and (4.11). In the real machine the currents are changing all the time and this examination gives only a good approximation for the saturation. The effects of the saturation are shown for inductances in figure 20.

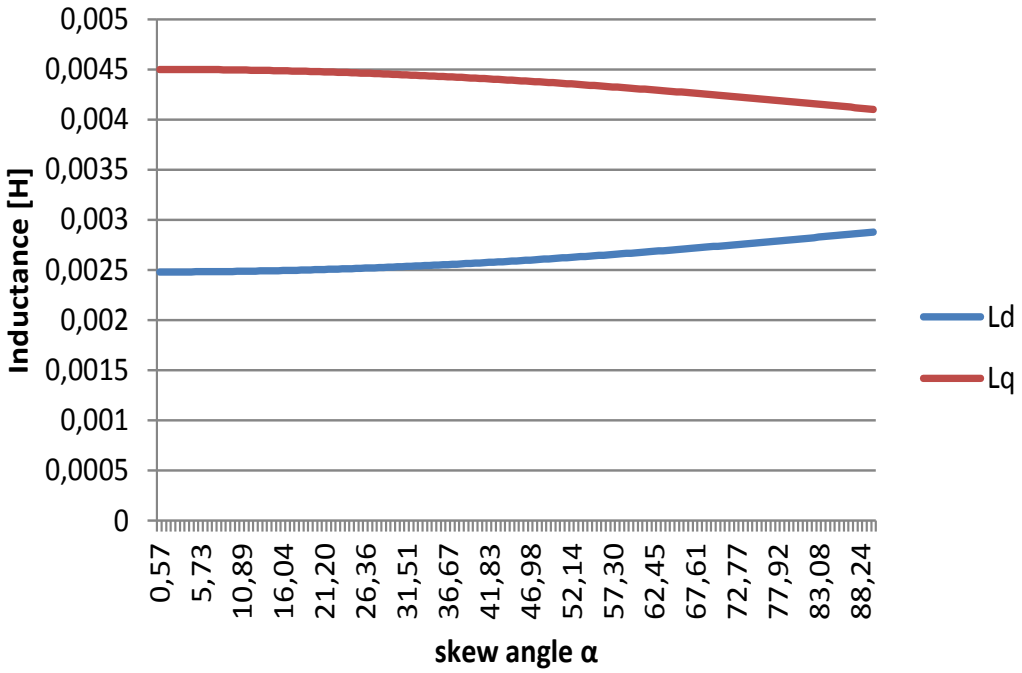

Figure 20 The effect of saturation for the inductances, current components are 5 A.

Figure 20 shows the synchronous inductances of the PMSM as a function of skew angle α. The values for the inductances L_d and L_q in equations (4.10) and (4.11) are taken from figures 16 and 17 assuming that the current components are 5 A. From figure 20 it can be seen that L_d is increasing and L_q is decreasing in the saturation. That is caused by the cross coupling effect. It is assumed now that the behaviour of the inductance curves is approximately the same as in figure 20 at all current values. At the same time when the d-axis inductance increases and the q-axis inductance decreases, the saliency ratio ε of the SynRaPMSM decreases. Figure 21 shows the behaviour of PM flux linkage as a function of the skew angle α.

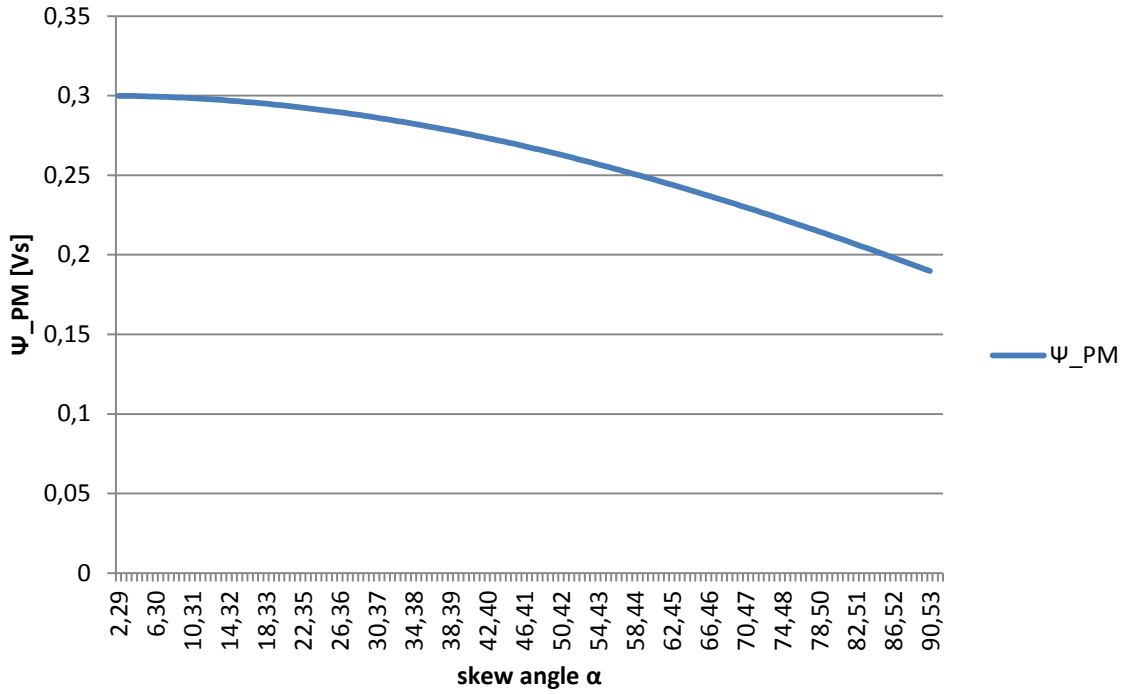

Figure 21 The behaviour of PM flux linkage as a function of the skew angle.

Figure 21 shows that the behaviour of the PM flux linkage ψ_{PM} as a function of skew angle is similar with the behaviour with current i_{q} as shown in figure 18. The flux linkage ψ_{PM} decreases also like the q-axis inductance. So the effect of cross coupling and saturation is now studied. The saturation model which is studied at chapter 4.3 is used in Microsoft Excel model.

4.4 Power capability of PMSM

The peak power capability over a wide speed range is only accessible with the control of the motor phase stator current magnitude and angle as written before at this study. With that kind of control MTPA-operation can be obtained over a variety of different loads and speeds. The rated voltage constraint at the motor terminals limits the output power capability at high rotational speeds. The stator voltage and the output power curves as a function of current angle γ for eight different motor speeds for one motor design are presented in figure 22.

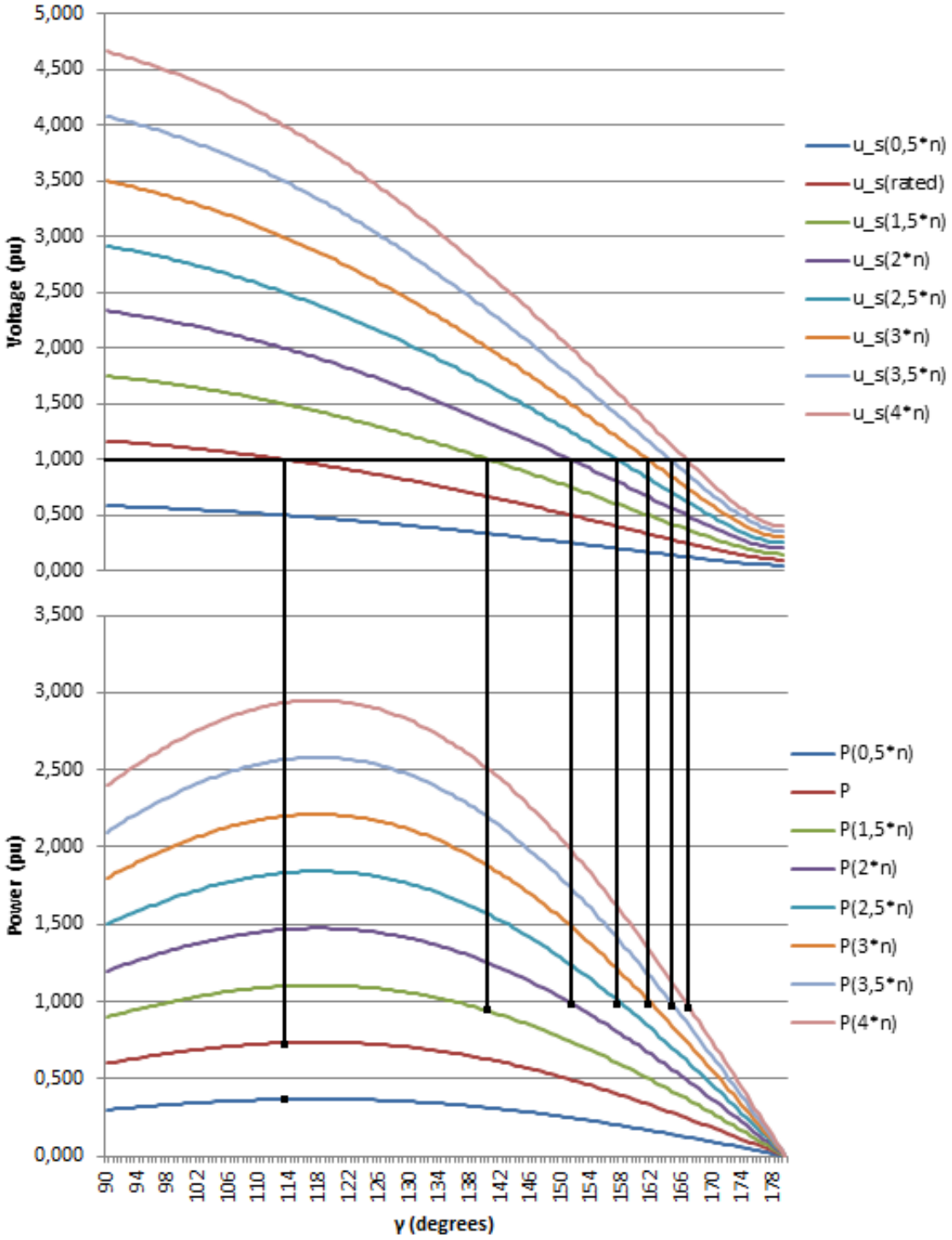

Figure 22 Stator voltage and output power as a function of the current angle for motor design ψ_{PM} = 0,6, L_d = 0,5 and L_q = 1. Stator current is 1 pu.

Figure 22 demonstrates the maximum output power with 1 pu voltage constraint. The PMSM makes full torque due to interaction with PM when the angle is 90°. With bigger angle the reluctance torque component starts to make torque also. In figure 22 it can be seen that when the current angle γ increases the stator voltage decreases. This is caused

by the d-axis armature reaction $\omega L_{\mathrm{d}} i_{\mathrm{s}} \cos\gamma$ from equation (2.47). The d-axis armature reaction is opposing the flux linkage caused by the permanent magnets ψ_{PM}. Correspondingly the q-axis armature reaction $\omega L_{\mathrm{q}} i_{\mathrm{s}} \sin\gamma$ decreases as the current angle gets nearer to 180°. In the figure also the maximum power with one per unit voltage constraint is shown. The voltage constraint does not prevent the motor operation at peak output power at low speeds but at high speeds the voltage constraint becomes more important.

Below the rated speed the voltage is less than 1 pu and the peak output power increases linearly with speed. It can be seen that the peak output power still increases after the one per unit speed is reached but no longer linearly with speed. The maximum power is reached at 2 pu speed. The power factor is one at that speed.

4.5 Combining the motor and inverter

When the motor and the machine are connected it is very important to know, how many coil turns the machine has in the stator. Number of coil turns will effect on the largeness of induced voltage. The equation of the induced voltage can be written according to Faraday's law

$$e = -\frac{d\psi}{dt} = -N\xi\frac{d\Phi}{dt}, \tag{4.13}$$

where N is number of coil turns, ξ winding factor and Φ magnet flux (Pyrhönen 2008). The effective value of induced voltage in sine form can be written

$$E = \frac{\hat{e}}{\sqrt{2}} = -N\xi\omega\hat{\Phi}. \tag{4.14}$$

The use of equation (4.14) demands that the peak value of magnet flux $\hat{\Phi}$ is known. The peak value of flux linkage can be calculated by knowing the pole pitch, characteristic length and the maximum value of magnet flux density in the airgap.

So the more coil turns in the stator, the more induced voltage. The machine with less stator coils is more efficient because the machine's output power gets lower when the induced voltage is big. So according to this the more torque is achieved by increasing coil turns. Feedback is that then the torque can be achieved only small speed range because the growth of induced voltage will decrease the power. Correspondingly the machine gives less torque but has high speed region when the machine is designed by using less coil turns. Basically the increasing of coil turns will affect the size of machine's inductances. Inductance can be written

$$L = \frac{N^2}{R_\mathrm{m}}, \tag{4.15}$$

where R_m is reluctance. For the inductance can be written also

$$L = \frac{\psi}{I} = \frac{N\Phi}{I}. \tag{4.16}$$

Previous equations show how the number of coil turns will affect also the inductances of the machine. When the inverter is matched in the motor and the inverter cannot give the designer enough current to reach the big enough torque, then number of coil turns should be increased. Otherwise if designer wants to reach higher speeds in the end of the machine operation, the number of coil turns should be decreased to fulfil demands. That depends really much on the application what kind of torque and speed demands are. The number of coil turns is not the only thing which will affect the characteristic of the machine. Thickness of coil and the number of parallel coil wires are also important things when the machine characteristics are optimized. Actually the number is not really important but the area which the huge number of parallel coils creates is important for the machine characteristics (Pyrhönen 2008).

5. FIELD WEAKENING POINT OF THE MACHINE

The field weakening point of the machine is determined by the program that is made by the Microsoft Excel according to the wish of one of the FiDiPRo project supporting companies. All the equivalent circuit parameters are needed to solve the problem. The calculation is done with per unit values because it is easier to work with them. In the end returning of the per unit values to the real values is done.

At the rated voltage and speed the pull-out torque of the machine depends on the inverse of the synchronous inductance and that is why the inductance should be low in order to get high torque. In the traction applications high torque is very advisable. In the permanent magnet machines this requirement is more important because the interior emf E_{PM} of the machine cannot be controlled. Usually the PM machines have 160 % pull-out torque at the rated voltage and speed. However, at lower speeds the torque is not as much inductance limited and higher torques can be achieved so more current can be used momentarily. All calculated results are directional but cannot be absolutely exact because of the saturation of the inductances.

In many works (Soong(a) et al. 2007), the rated speed was chosen to be the highest speed at which the rated torque could be produced. In this thesis the 1 pu speed is chosen to be the maximum speed n_{max} in the constant power speed range in the beginning of the program. That is done because the task is to define the speed which gives the rated torque and that speed is totally unknown, so it cannot have any reasonable value at the start of the problem. At this speed of the machine field weakening process starts.

The other two design parameters for modelling the machine characteristics in the field weakening range will be the saliency ratio ε and the maximum induced voltage E_{max}. Those design parameters are selected because they are independent of machine's rated speed.

The equations for the design parameters, which helps to define the physical induced voltage ψ_{PM}, and the d- and q-axis inductances L_{d} and L_{q} are presented next.

$$\varepsilon = \frac{L_{\mathrm{q}}}{L_{\mathrm{d}}} \rightarrow L_{\mathrm{q}} = L_{\mathrm{d}}\varepsilon, \tag{5.1}$$

$$I_{\mathrm{x}} = \frac{\psi_{\mathrm{PM}}}{L_{\mathrm{d}}} \rightarrow L_{\mathrm{d}} = \frac{\psi_{\mathrm{PM}}}{I_{\mathrm{x}}}, \tag{5.2}$$

$$E_{\mathrm{PM,max}} = \omega_{\max}\psi_{\mathrm{PM}} \rightarrow \psi_{\mathrm{PM}} = \frac{E_{\mathrm{PM,max}}}{\omega_{\max}}. \tag{5.3}$$

The three equations above are used to solve the physical rated electrical angular frequency which helps one to define the field weakening speed in per unit values.

5.1 Implementation of the program

The program designing is started on the assumption that the point of the field weakening can be settled down with adjusting the frequency f, electrical angular frequency ω and mechanical angular frequency Ω. For the torque as a function of mechanical angular frequency can be written as

$$T(\Omega) = \begin{cases} T_{\mathrm{n}} \quad , \ \Omega < \Omega_{\mathrm{n}} \\ T_{\mathrm{n}} \frac{\Omega_{\mathrm{n}}}{\Omega}, \ \Omega \geq \ \Omega_{\mathrm{n}} \end{cases} \tag{5.4}$$

For the voltage it can be written same way by controlling the flux linkage at a constant value below the rated speed and proportional to $1/\omega$ above rated electrical frequency. The voltage equation differs from previous thus that now the changing parameter is an electrical angular frequency. The voltage equation

$$U(\omega) = \begin{cases} U_{\mathrm{n}} \frac{\omega_{\mathrm{n}}}{\omega}, \ \omega < \omega_{\mathrm{n}} \\ U_{\mathrm{n}} \quad , \ \omega \geq \omega_{\mathrm{n}} \end{cases} \tag{5.5}$$

The behaviour of the torque line and the voltage line is expressed by the equations (5.4) and (5.5).

A point where the field weakening starts can be defined by knowing the slope of the voltage line and the trajectory of torque. When the slope is bigger than one the motor voltage at the base operating point decreases and accordingly when the slope is smaller than one the voltage at the base operating point increases. The point where the field weakening process starts is obtained from the crossing point of MTPA- and FW-control strategy. The equation for the point is

$$\omega_{\mathrm{FW}} = \frac{u_{\mathrm{s,max}}}{\sqrt{(R_{\mathrm{s}} i_{\mathrm{q\_MTPA}} + \psi_{\mathrm{PM}} + L_{\mathrm{d}} i_{\mathrm{d\_MTPA}})^2 + (R_{\mathrm{s}} i_{\mathrm{d\_MTPA}} - L_{\mathrm{q}} i_{\mathrm{q\_MTPA}})^2}}. \tag{5.6}$$

This means that there is no single field weakening point but it depends on the torque. Equation (5.6) is used with real values because part of the base values are unknown. That is why some of the per unit values are also unknown. After the electrical angular frequency is known, one wants to know the rotational speed when the field weakening process starts. The field weakening frequency can be calculated by

$$f_{\mathrm{FW}} = \frac{\omega_{\mathrm{FW}}}{2\pi}. \tag{5.7}$$

The rotational speed and the frequency have following dependence

$$n_{\mathrm{FW}} = \frac{f_{\mathrm{FW}}}{p}. \tag{5.8}$$

Now the rated rotational speed of the machine and the rated frequency are known and all the rest of the base values can be calculated. After that all the base values are calculated, the calculation is transferred to the per unit values because it is easier to work with those.

Because at the start the user does not know the machine's rated speed, one need to organize the parameters again when the field weakening speed is known. That can be done with the help of the speed ratio. The speed ratio *s* can be calculated from the real values of the machine

$$s = \frac{n_{\mathrm{max}}}{n_{\mathrm{FW}}}. \tag{5.9}$$

When the speed ratio is known everything is needed to be scaled with it. After scaling the nominal rotational speed is 1 pu and the maximum rotational speed is as large as the speed ratio. Now everything can be calculated normally with the per unit values.

If the machine operation needs the MTPV-control then the user must know the speed reference to begin MTPV. Equation for that speed is

$$\omega_{\mathrm{MTPV}} = \frac{u_{\mathrm{s}}}{\sqrt{(R_{\mathrm{s}} i_{\mathrm{q\_MTPV}} + \psi_{\mathrm{PM}} + L_{\mathrm{d}} i_{\mathrm{d\_MTPV}})^2 + (R_{\mathrm{s}} i_{\mathrm{d\_MTPV}} - L_{\mathrm{q}} i_{\mathrm{q\_MTPV}})^2}}. \tag{5.10}$$

In equation (5.10) the d- and q-axis current components are such that the magnitude of the total stator current i_s = 1. Then the FW-control ends and the MTPV-control method takes place. The maximum output power can be produced now in all speed ranges considering both the voltage and the current limits.

The base knowledge for that program is that the stator flux linkage ψ_s = 1 pu, I_s = 1 pu and U_s = 0.9 pu. For the voltage reserve is left 10 % but the user can change the amount of the voltage reserve freely.

5.2 The flowchart of the program

Now when all the equations of the program are fully presented, the process can be presented with a flowchart which is presented in figure 23.

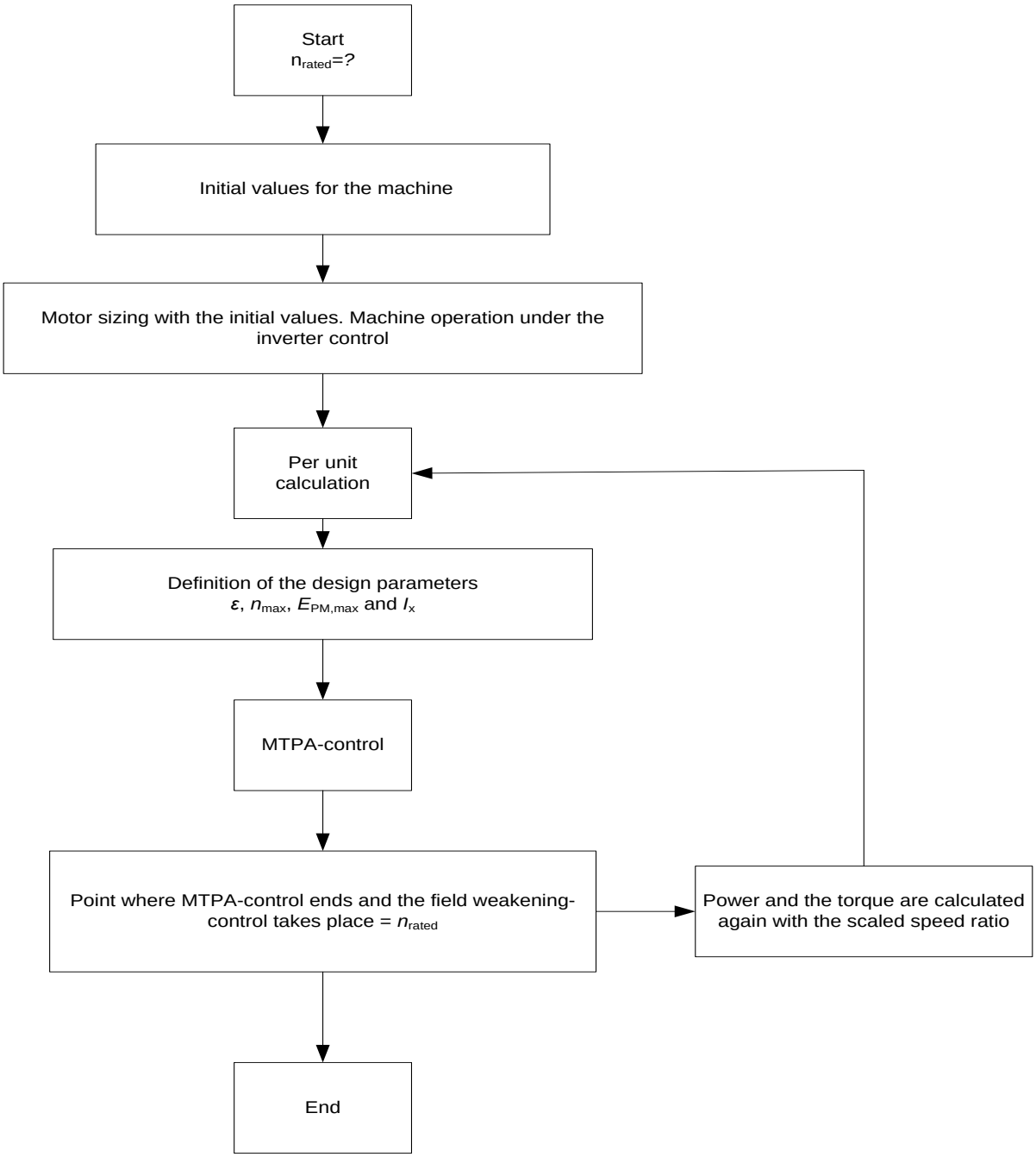

Figure 23 Flowchart of the program that defines the point where the field weakening starts.

The choice of the optimum speed ratio is one of the most important things in this program. This analysis of the PMSM performance as a function of the speed ratio is important for the designers because the analysis shows how the machine works at different speeds. Other given parameters for the design are the maximum speed $n_{\max}$, the stator voltage u_s and the stator current i_s. Also the minimum speed should be given $n_{\min}$ so that the program knows for how long the maximum torque should be used at the start. The parameters that will change according to every operation state are the induced voltage caused by

the permanent magnets E_{PM}, inductances multiplied with electrical angular frequencies ωL_d and ωL_q. The current components will change, too, but the magnitude of current is always the same except during very low speeds when a large amount of extra torque is needed for a short period of time. The inverter is used at the start to get more torque at very short time to get the vehicle moving.

The program is operable also without real values if the user wants to use pu-values directly. Then the start of the program's flowchart (figure 23) is different but the rest of the program is working under the same principles.

6. RESULTS

In this chapter the results are presented. Three example machine designs are presented to show the functionality of the machine in different operation conditions. Part of the next figures are drawn by Matlab to help one understand graphically the behaviour of the current vector in each operation state. The same result will be analytically solved by the Microsoft Excel. Figure 24 shows the motor at different operation states for design where parameters ψ_{PM} = 0.34 pu, saliency ratio ε = 2.82, L_d = 0.416 pu and the characteristic current of the machine is I_x = 0.82 pu. The maximum speed is 7.25 pu after the speed is scaled with the speed ratio. The stator voltage is now 0.95 pu.

The blue circle in the figure is the current circle, red ellipses represent the ratio between the voltage and the speed, green lines are the constant torque lines and the black curve represents the current vector at optimal current angle γ.

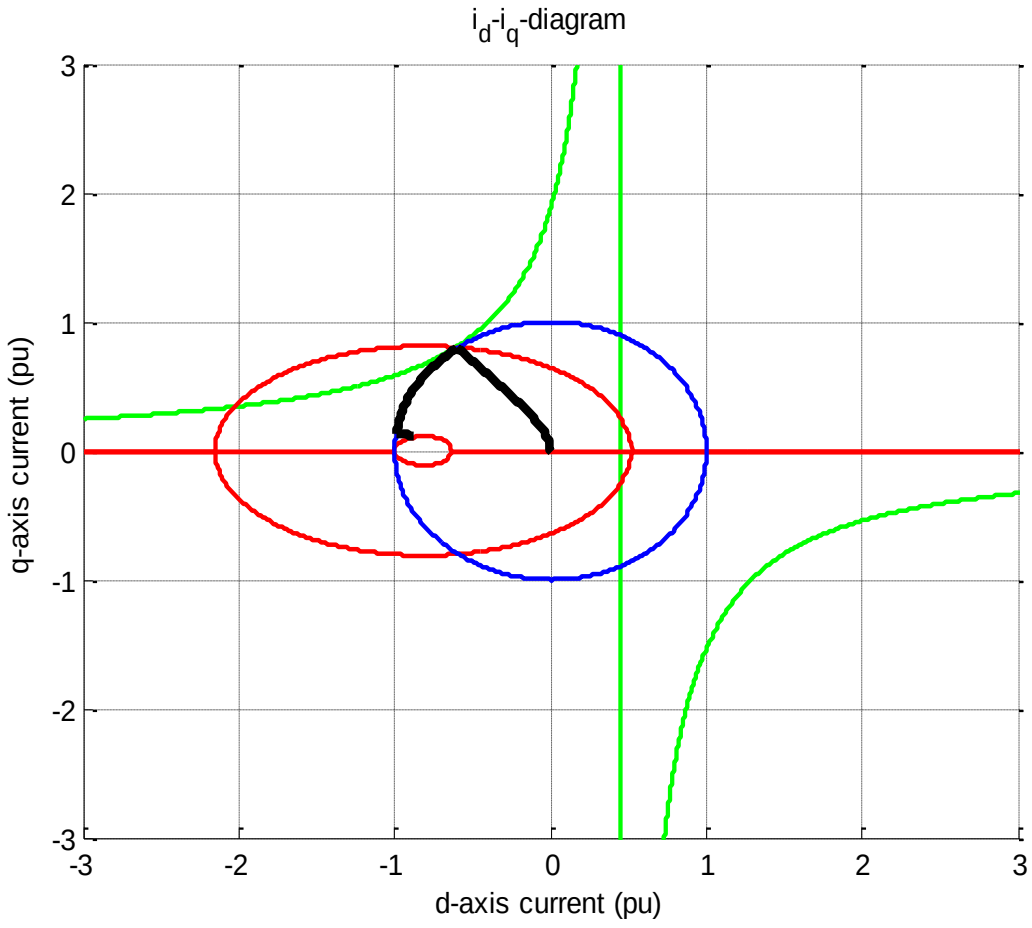

Figure 24 Operation trajectories of SynRaPMSM with design parameters ψ_{PM} = 0,34 pu, ε = 2.82, L_d = 0.416 pu, I_x = 0.82 pu and n_{max} = 7.25 pu. Stator voltage is 0.95 pu.

Figure 24 presents such a machine design that will use all the control methods to control the current vector. This kind of a machine structure has a relatively big speed range. The machine structure is also cheap because of the less amount of magnet material in the rotor. The maximum induced voltage of this machine can be calculated by using equation (5.3). The maximum induced voltage is 2.47 pu and one can see that it is 2.6 times u_s. So the induced voltage is quite big.

In figure 24 it can be seen also that the voltage limit of the machine comes against so that the current vector cannot be controlled anymore. The variation of the current components in terms of machine's speed is shown in figure 25. The d-axis current is negative but in figure 25 is presented the magnitude of i_d.

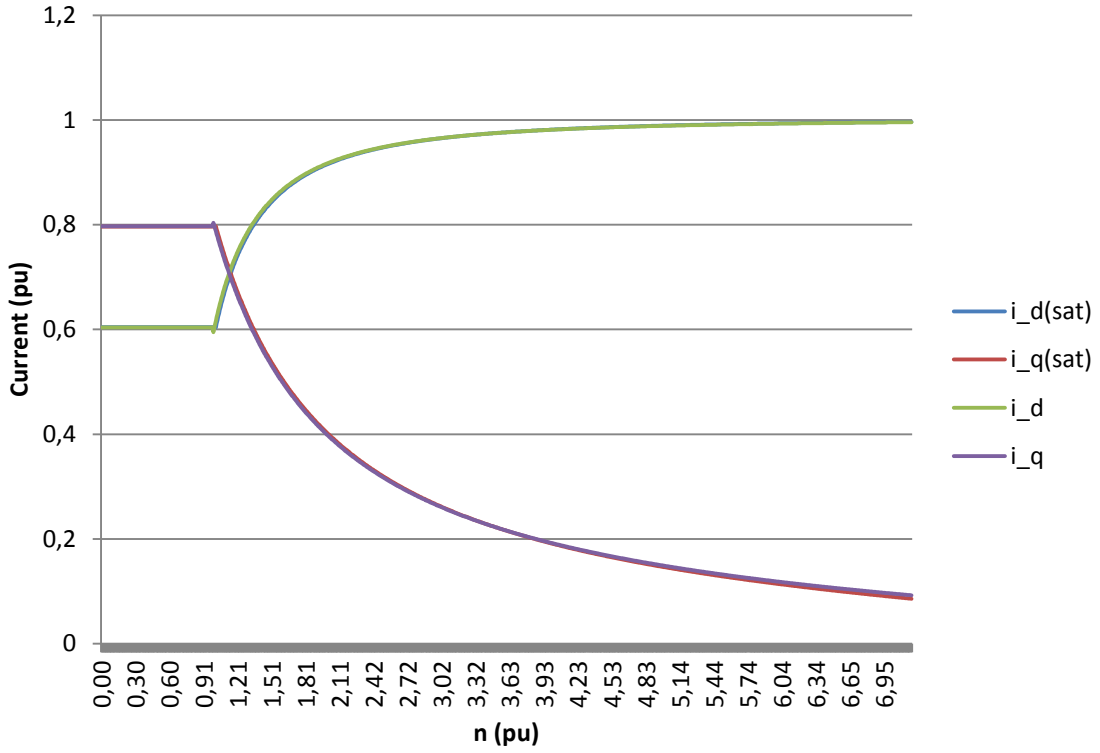

Figure 25 Variation of current components as a function of speed. Current i_d is presented by using its magnitude while its absolute value is normally negative.

Currents in figure 25 are shown so that the magnitude of the stator current is always in its nominal value which is 1 pu. Before the field weakening process the current components are kept under MTPA-control and hence i_d and i_q are constants. When the field weakening starts FW-control takes place and the demagnetization of the stator flux starts. The magnitude of d-axis current increases and correspondingly the magnitude of q-axis current decreases. Figure 25 shows also the behaviour of the current components when inductances will saturate. One notices that there are only minor differences in the field weakening

but hardly noticeable. The torque and the power characteristics in terms of speed are presented in figure 26.

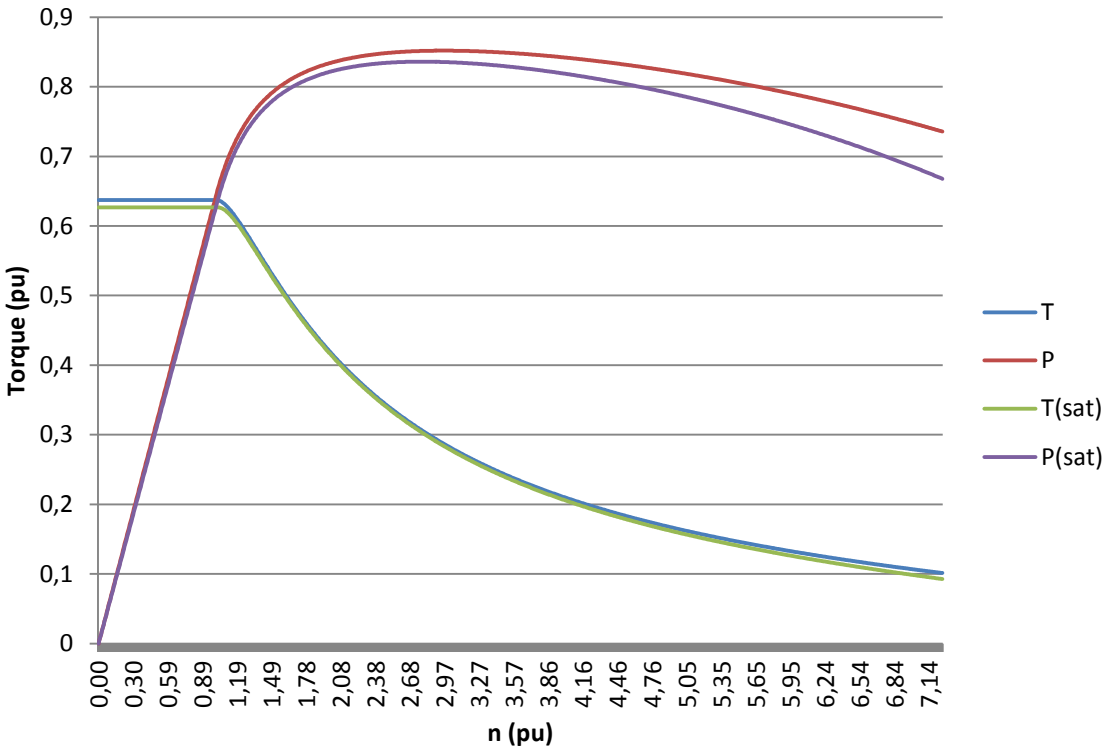

Figure 26 Torque and power as a function of rotational speed for the previously presented design parameters.

In figure 26 it can be seen that the torque is constant in the constant flux range. When the field weakening starts the torque starts to decrease. When the voltage of the motor has reached its rated value the field weakening starts. The mechanical power of the motor is increasing linearly in the constant flux range and continues its growing in the field weakening range always till the deep field weakening and gets near to the 0.85 pu power. The theoretical power limit is 1 pu and to get that power the motor should rotate at infinite speed. It is noticeable that the power starts to weaken at half of the speed range which is caused by the relatively small flux linkage of PM.

It is noticeable also, how the saturation of inductances affect the lines of the torque and power. One can see in figure 26 that the field weakening point of the machine has moved now a little bit over of 1 pu speed in the saturation case. The lines of torque and power are similar but the saturation of the inductances causes small torque and power drops. Figure 27 shows the machine operation with the inverter allowing maximum current of 1.7 pu.

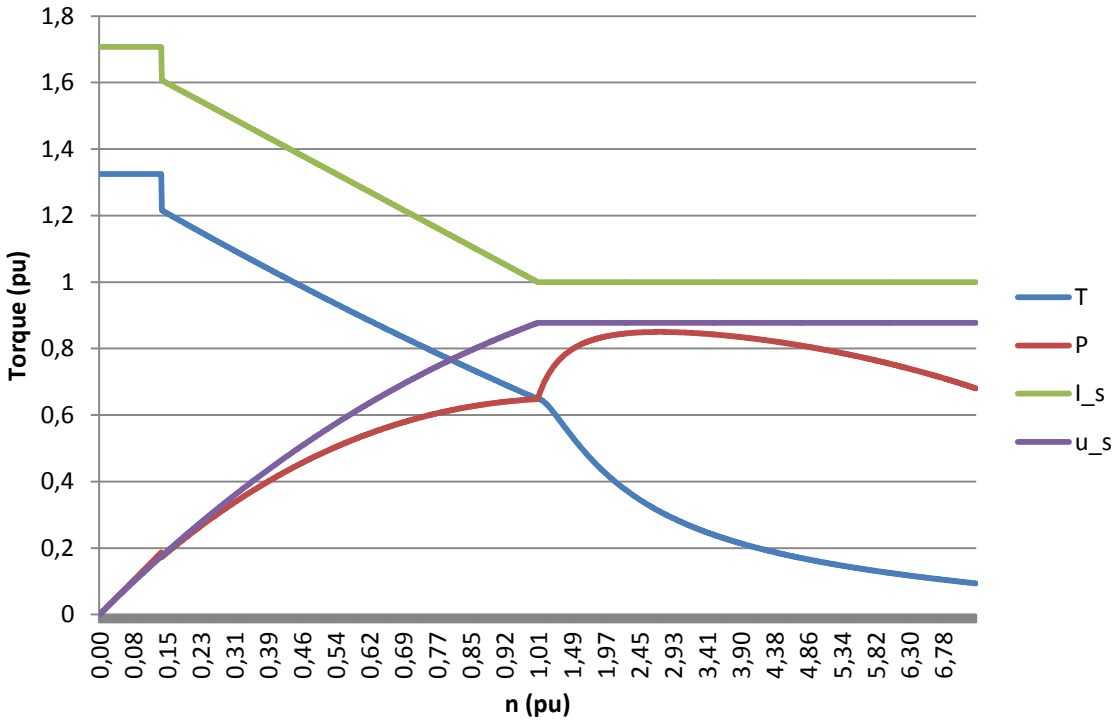

Figure 27 Machine with inverter at wide speed range.

Figure 27 illustrates the lines for the torque, power, current and voltage. In figure 27 it can be seen that the inverter is used to the start where a large amount of torque is needed. After start the MTPA-control is continued to drive the machine at its rated current. When the field weakening point has been obtained, the FW-control starts. It can be seen that when the FW-control starts, more power is gained. The inverter is now fitted in the motor and the current vector line produces torque over the whole speed range.

Another machine design which is examined next has the following design parameters: L_d = 0,3 pu, ε = 3, ψ_{PM} = 0,8 and I_x = 2,67 pu. Stator current and the stator voltage are both 1 pu. Saturation is not considered with this machine design. Figure 28 shows the machine operations in i_d-i_q-diagram.

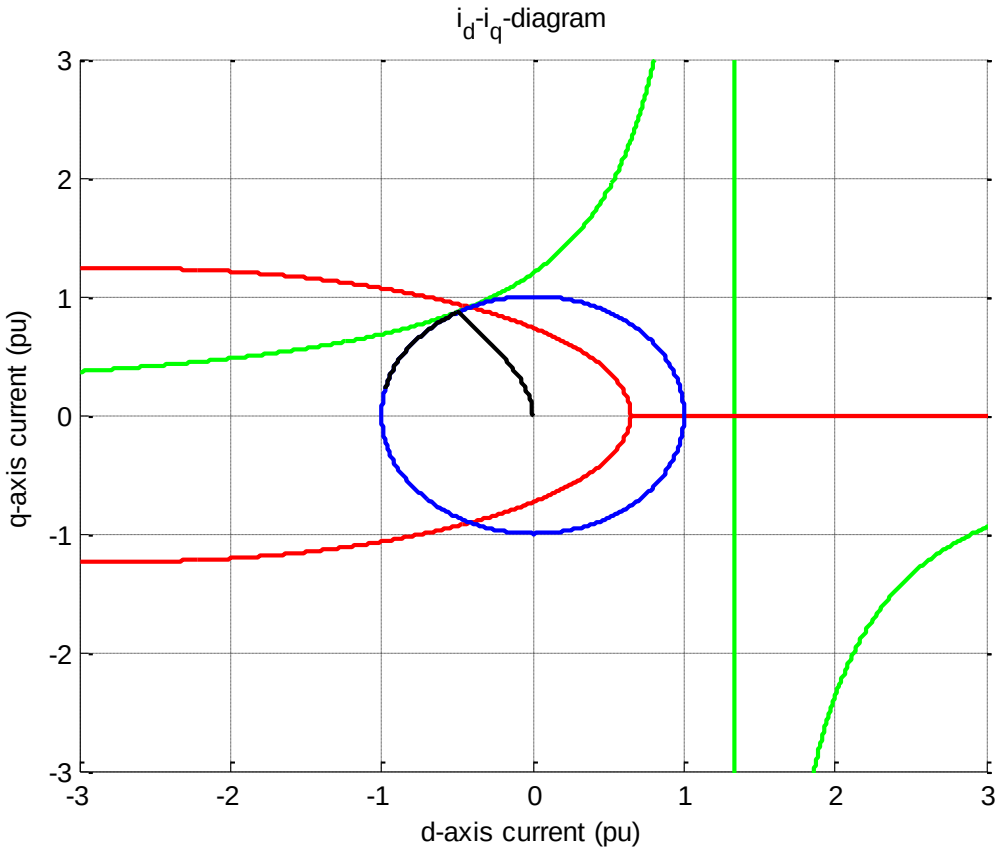

Figure 28 Current-diagram which shows the machine operations at the different operation states.

In figure 28 one can see the machine at two different operation states (black line): MTPA and the field weakening. It can be seen also that MTPV-control strategy does not exist because $\psi_{PM}/L_d > i_{max}$. Current variation has been shown in figure 29 as a function of speed. The d-axis current is presented with its magnitude.

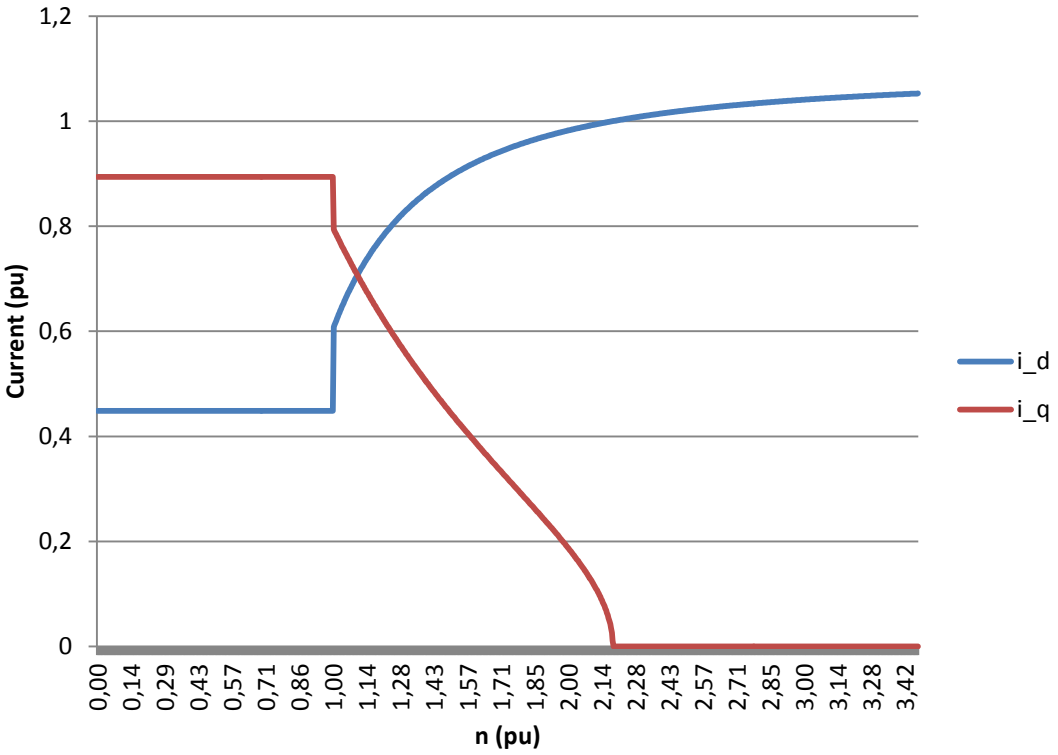

Figure 29 Current variation as the function of speed for the second machine design. Current i_d is presented by using its magnitude while its absolute value is normally negative.

Figure 29 shows the d-axis and the q-axis currents in terms of the speed. The collapse of the q-axis current will cause the vanishing of the torque as can be seen later. This is due to that the PM material is lying on the d-axis and when there is no q-axis current available the cross field principle is not fulfilled and hence no more torque or power are available. The torque and the power for this machine design in terms of speed can be seen in figure 30.

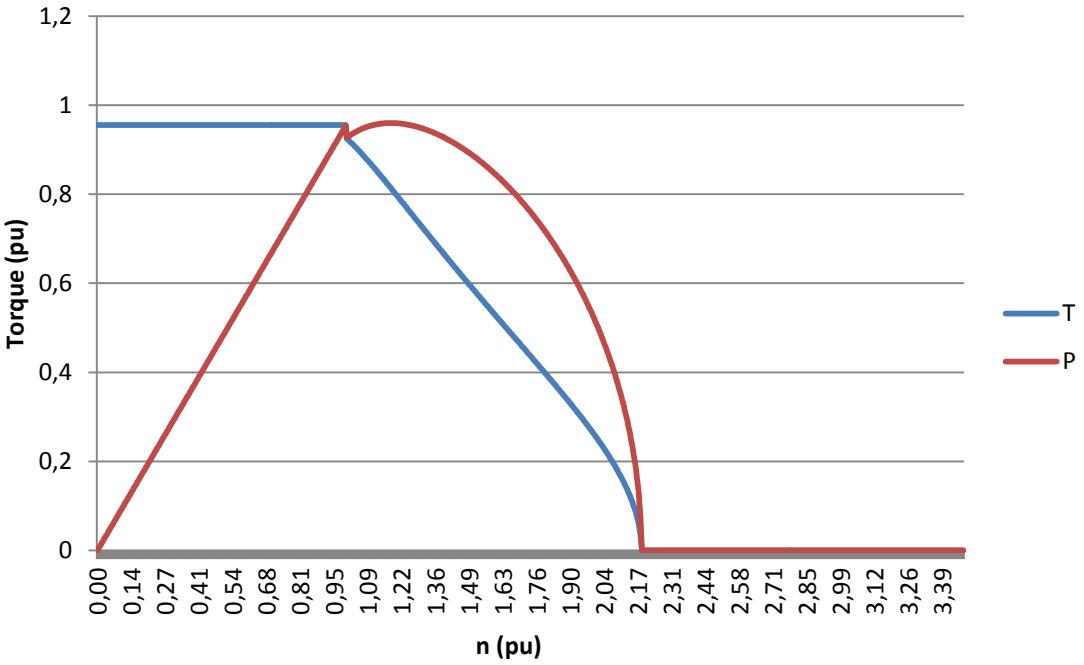

Figure 30 The torque and the power as function of the speed for the previous machine design.

In figure 30 it can be seen that the torque will decrease to the zero when i_q-current is no available. That can be seen from the torque equation (2.41). This machine design is very poor because with such a machine it is not possible to achieve the wanted maximum speed. But in some drive which is used at constant speed and hence it needs only a small speed range it can be used. Power is over 0.9 pu close to the rated speed.

The last example machine has a smaller saliency ratio than the previous machines. The values for the calculation are L_d = 0,4 pu, ε = 1,62, ψ_{PM} = 0,617 pu, I_x = 1,52 pu and n_{max} = 2,38 pu. Figure 31 shows the controlling of the current vector with the help of current diagram.

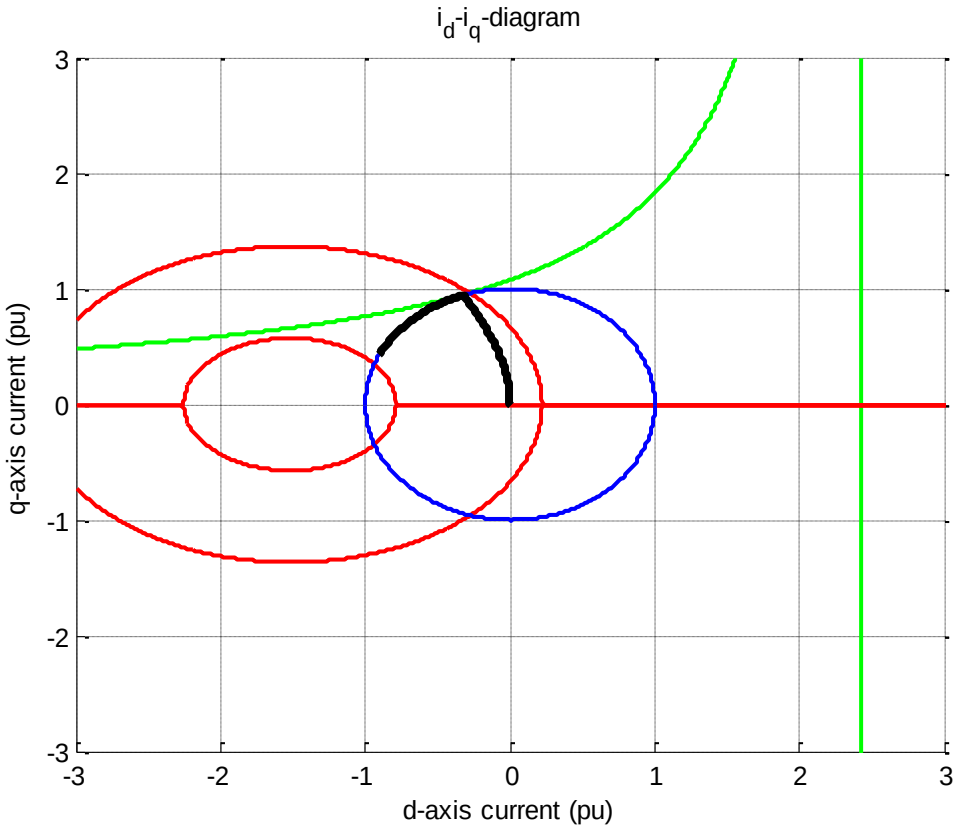

Figure 31 i_d-i_q-diagram which presents the machine in different states.

Figure 31 illustrates the control modes of the machine until it is driven close to the voltage limit. For the voltage reserve is left in this case 10 %, so the stator voltage u_s = 0.9 pu. One can notice that the machines characteristic current is now bigger than 1 pu, so the MTPV-line lies outside the current circle. This machine suits to the drive which does not need very large speed range for example city traffic or work vehicles. Magnitude of both current components is presented in figure 32 in terms of the machine's speed.

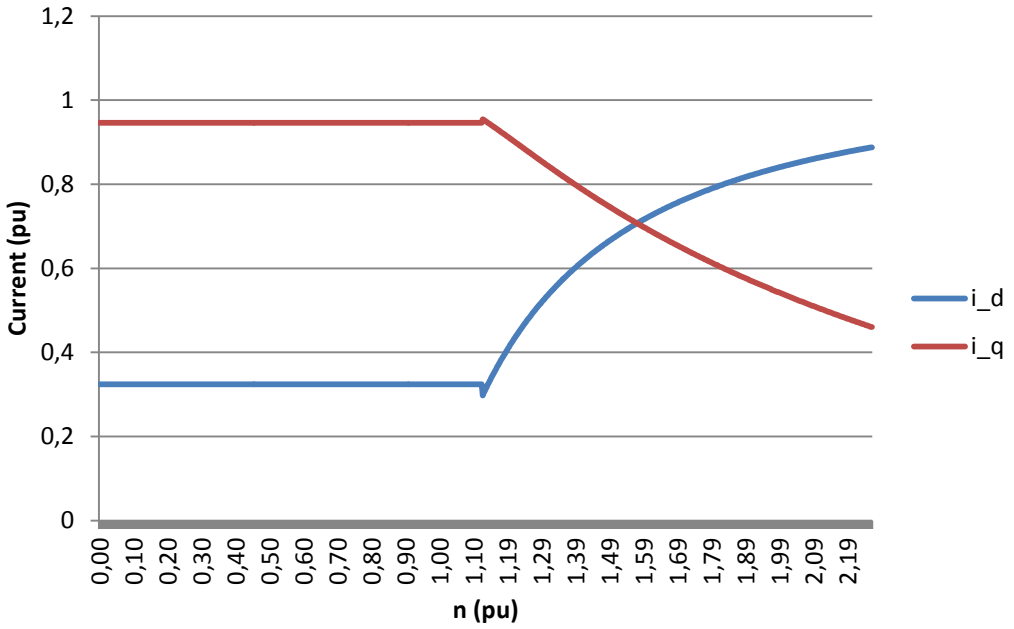

Figure 32 Current components as the function of machine's rotational speed of the previously presented machine. Current i_d is presented by using its magnitude while its absolute value is normally negative.

Now the field weakening starts approximately at halfway of the machines speed range as one can see in figure 32. At the end of the machine operation this machine design has a relatively large torque as one can notice from the i_q-current which is still as large as 0.45 pu. The torque and power are presented in figure 33 as the function of rotational speed.

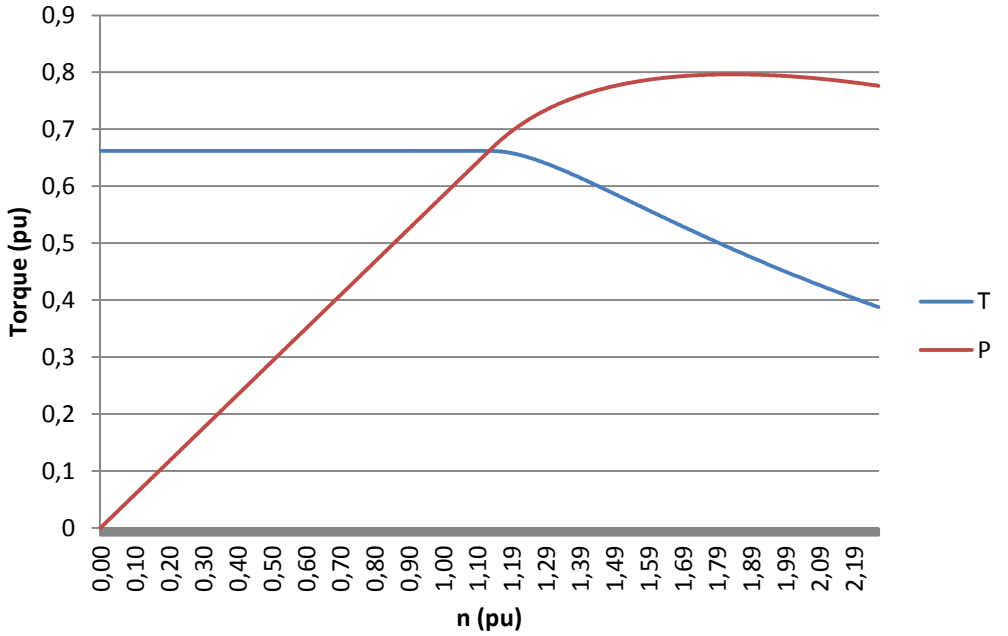

Figure 33 Torque and the output power as a function with speed.

In figure 33 it can be seen that the machine with previous parameters does have large torque at the end. If one wants to increase the maximum speed of the third machine design the power will start to collapse very quickly. The saliency ratio should be bigger, if one wants to use this machine in very high speeds. Figure 34 shows the machine with a big starting current (2.1 pu) in the inverter control.

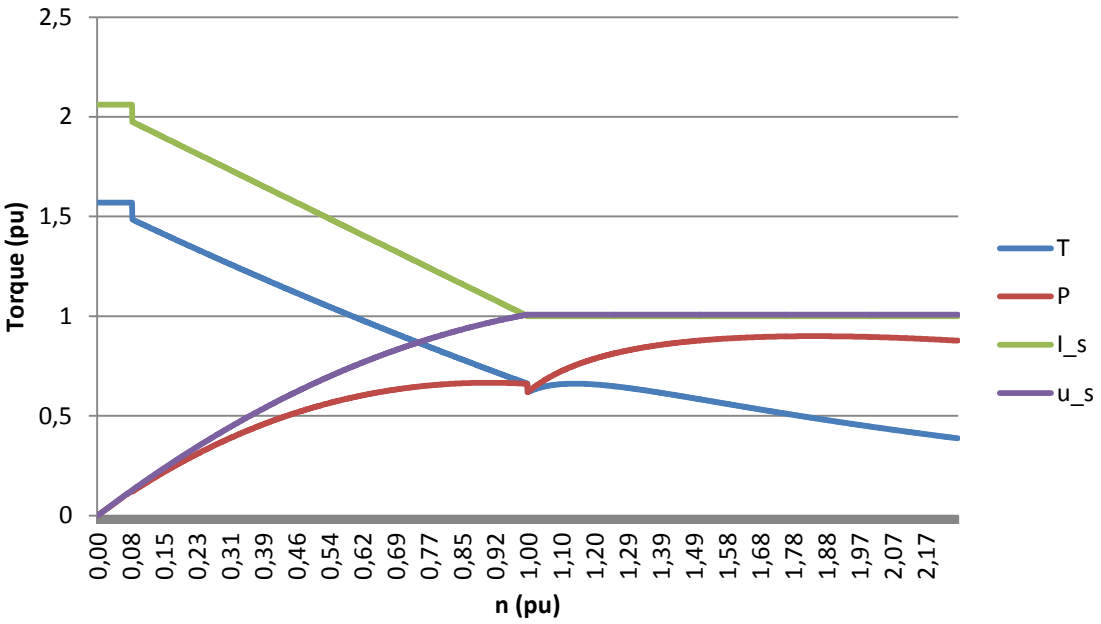

Figure 34 Machine operations at start-up to the end with current boost in the beginning.

In Figure 34 the starting current is large approximately 2.1 pu and the torque at start is also large. The inverter should be selected so that it can produce 2.1 pu current to get 1.6 pu torque.

The saliency ratio should be as big as possible because a bigger reluctance torque should give a bigger output power, especially, at lower speeds and also at higher speeds since the d-axis demagnetizing effect has increased and then the reluctance torque is more available. Inductances should be selected so that the saliency ratio is near to the value 3 pu.

With the work tool, one can notice that the typical values for the d-axis inductance L_d = 0.2…0.5 pu and q-axis inductance L_q = 0.6-1.2 pu. Hence, the machine can produce the torque over the wide speed range. If the inductances differ much from those values that are previously presented, the machine cannot work correctly by its means. The effect of the stator resistance is hardly noticeable and it has a significant effect only at very small

voltages and high torques. In the vicinity of the field weakening point, the stator resistance does not have any significant effect. Hence, under high speeds the stator resistance can be neglected. If the machine inductances are chosen really big, the machine's rotational speed starts to reach infinity. In the end let's take one example where the inductances are relatively small and the machine is driven over 1 pu current in the field weakening region. That process is presented in the figure 35.

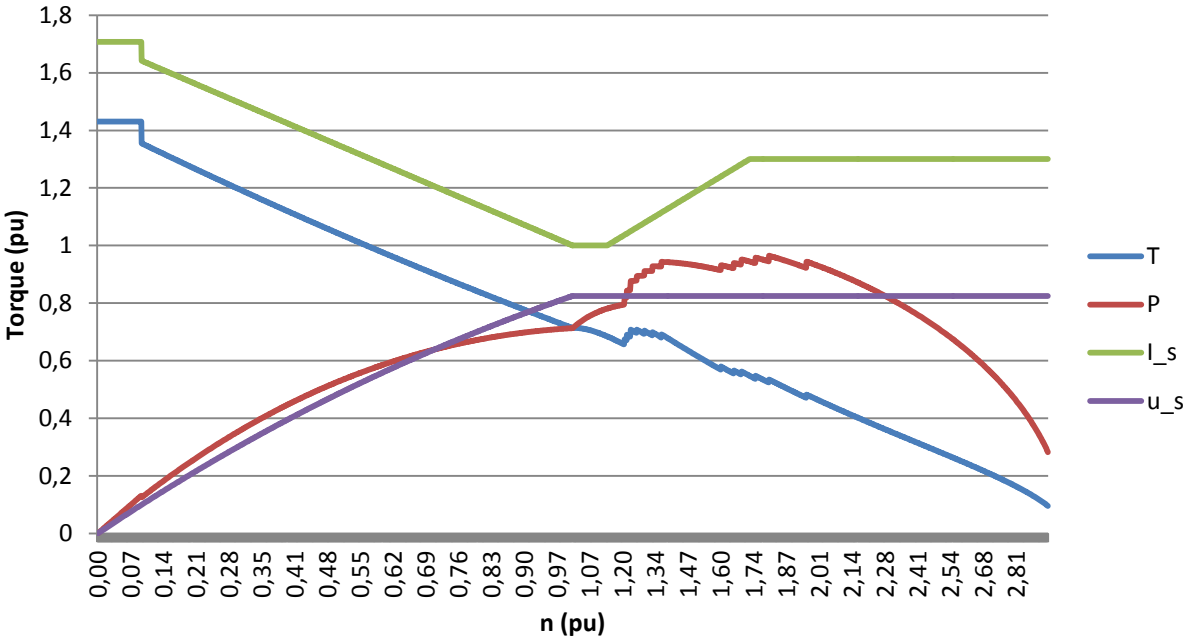

Figure 35 Field weakening operation when the motor with relatively low inductances is driven over 1 pu current in field weakening region.

In figure 35 can be seen that the power and torque can be achieved if the motor is driven over 1 pu current. The machine parameters are: L_d = 0.26 pu, L_q = 0.68 pu and ψ_{PM} = 0.61 pu. It can be seen that in the field weakening the machine cannot be driven long time over current limit because then the machine will heathen too much. It is seen that even with low inductances machine can operate at full speed range. Hence this proves that if inductances are really big the speed starts to increase towards infinity without using current which is bigger than the current limit. In the end of machine operation it can be seen that the current is limited to 1.3 pu value. In theory this would be optimal way to drive the motor but in practice this kind of use is impossible during a long time. Machine can be driven over current limit only very short time in field weakening.

7. CONCLUSION

The actions of permanent magnet synchronous machine in field weakening process are studied in this thesis. A detailed analysis of the flux control with different control methods for the wide speed range has been presented. The work tool, equations and methods of defining the field weakening point are discussed. The main target of this thesis was to solve the field weakening point for the SynRaPMSM which is used in traction applications but the solving methods of field weakening point can be used other PM machines as well as SynRaPMSM.

The machine operations are studied widely in the large speed range. One noticed that the effect of the stator resistance is very small and it will impact only in the start when the stator voltage is small. The approximation of the saturation is difficult without any measurements and so the results with the saturation model are only directional but not exact. The work tool was implemented by per unit values because then the amount of parameters has been decreased and the comparison of changing parameters is easier.

The point where the field weakening starts has been achieved at the crossing point of the MTPA- and the field weakening control. Machine operations with different L_{d}, L_{q} and ψ_{PM} are studied and the effect of machines saliency is examined. The analysis of the output power and the output torque is done when the wanted speed is achieved. The constant power curve for the inverter operation is plotted and analysed. A big starting torque is needed to get the vehicle moving. The inverter should be chosen so that it can produce the current needed for the given starting torque.

Overall this thesis will give a good vision for that how the machine should be designed for traction applications but lots of measurements still need to be done because the saturation part is only approximate and strongly dependent at which position the magnets are placed in the rotor. Saturation of traction motors would be a good research subject in the future.

REFERENCES

Chizh, A. 2010. Permanent Magnet Synchronous Machine for Parallel Hybrid Vehicle. Master's thesis. Lappeenranta University of Technology

Kaukonen, J. 1999. Salient Pole Synchronous Machine Modelling in an Industrial Direct Torque Controlled Drive Application. Diss. Lappeenranta University of Technology. ISBN 951-764-305-5

Mohan, N. Undeland, T.M. Robbins, W.P. 2003. Power Electronics: Converters, Applications and Design. John Wiley & Sons, Ltd. ISBN: 0-471-22693-9. Third edition.

Neorem Magnets. [webdocument]. [cited 26.5.2011]. Available at http://www.neorem.fi/products/permanent-magnets/

Parviainen, A. 2005. Design of Axial-flux permanent magnet low-speed machines and performance comparison between radial-flux and axial-flux machines. Diss. Lappeenranta University of Technology. ISBN 952-214-030-9

Pyrhönen, J. 2009 Lecture notes in course electrical drives.

Pyrhönen, J. Jokinen, T. Hrabovcova, V. 2008. Design of Rotating Electrical Machines. John Wiley & Sons, Ltd. ISBN: 978-0-470-69516-6

Ruoho, S.2011 Modeling Demagnetization of Sintered NdFeB Magnet Material in Time-Discretized Finite Element Analysis. Aalto University publication series, ISBN 978-952-60-4000-4

Conference papers

Aydin, M. Huang, S. Lipo, T. A. 2010. Design, Analysis and Control of a Hybrid Field-Controlled Axial-Flux Permanent-Magnet Motor. IEEE Trans. Ind. Vol. 57, No. 1, Jan p. 78-87

Chy, M. I. Uddin, N. 2007. Analysis of Flux Control for Wide Speed Range Operation of IPMSM drive. IEEE. Ontario, Canada, P. 256-260

Hall, E. Balda, J. C. 2002. Permanent Magnet Synchronous Motor Drive for HEV Propulsion: Optimum Speed Ratio and Parameter Determination. IEEE p. 1500-1504

Haque, M. E. Zhong, L. Rahman, M. F. 2002 Improved Trajectory for an Interior Permanent Magnet Synchronous Motor Drive with Extended Operating Limit. Journal of Electrical and Electronic Engineering. Institute of Engineers. Australia. Vol 22, No. 1, p 49-57

Haque, M. E. Zhong, L. Rahman, M. F. 2002. Improved Trajectory Control for an Interior Permanent Magnet Synchronous Motor Drive with Extended Operating Limit. Journal of Electrical and Electronics Engineering, Australia, vol22(1), p. 49-57

Ilioudis, V. C. Margaris, N. I. 2010. Flux Weakening Method for Sensorless PMSM Control Using Torque Decoupling Technique. Conf. Rec. IEEE, Thessaloniki, Greece, July 9-10, p. 32-39

Lindh, P. Rilla, M. Jussila, H. Nerg, J. Tapia-Ladino, J. A. Pyrhönen, J. 2011. Interior permanent magnet motors for traction application with non-overlapping concentrated windings and with integer slot windings. IREE Vol. 6. No. 4

Luise, F. Odorico, A. Tessarolo, A. 2010. Extending the Speed Range of Surface Permanent-Magnet Axial-Flux Motors by Flux-Weakening Characteristic Modification. Conf. Rec. ICEM, Rome, Italy, Sep 6-8

Meyer, M. Grote, T. Böcker, J. 2007 Direct Torque Control for Interior Permanent Magnet Synchronous Motors with Respect to Optimal Efficiency. Power electronic and applications. ISBN: 978-92-75815-10-8. Aalborg, Denmark. p. 1-9

Schiferl, R. F. Lipo, T. A. 1990. Power Capability of Salient Pole Permanent Magnet Synchronous Motors in Variable Speed Drive Applications. IEEE Trans. Ind. Appl. Vol. 26 No. 1, Jan/Feb p. 115-123

Soong(a), W. L. Han, S. Jahns, T. M. 2007. Design of Interior PM Machines for Field-Weakening Applications. Conf. Rec. ICEM, Seoul, Korea, Oct 8-11, p. 654-664

Soong(b), W. L. Reddy, P. B. El-Refaie, A. M. Jahns, T. M. Ertugrul, N. 2007. Surface PM Machine Parameter Selection for Wide Field-Weakening Applications. IEEE p. 882-889

Takahashi, I. Noguchi, T. 1986. A New Quick-Response and High-Efficiency Control Strategy of and Induction Motor. IEEE Trans. Ind. Appl. Vol. IA-22 (1986), p. 820-827

Zhu, Z. Q. Li, Y. Howe, D. Bingham, C. M. Stone, D. 2007. Influence of Machine Topology and Cross-Coupling Magnetic Saturation on Rotor Position Estimation Accuracy in Extended Back-EMF Based Sensorless PM Brushless AC Drives

Zhu, Z. Q. Qi, G. Chen, J. T. Howe, D. Zhou, L. B. Gu, C. L. 2009. Influence of Skew and Cross-Coupling on Flux-Weakening Performance of Permanent-Magnet Brushless AC Machines. IEEE Transactions on Magnetics. Vol. 45 No. 5, May p. 2110-2117

APPENDIX

Appendix 1. Per unit values

The use of per unit values is justified with electrical machines because they show directly the relative magnitude of a certain parameter. Per unit values were used in defining of the field weakening point. Per unit values can be obtained by dividing each dimension by a base value. Let us define base values first

$$U_\mathrm{b} = \frac{\sqrt{2}U_\mathrm{N}}{\sqrt{3}},$$

$$I_\mathrm{b} = \sqrt{2}I_\mathrm{N},$$

$$\omega_\mathrm{b} = 2\pi f_\mathrm{N} = \omega_\mathrm{N},$$

$$Z_\mathrm{b} = \frac{U_\mathrm{b}}{I_\mathrm{b}} = \frac{U_\mathrm{N}/\sqrt{3}}{I_\mathrm{N}},$$

$$L_\mathrm{b} = \frac{Z_\mathrm{b}}{\omega_\mathrm{b}} = \frac{U_\mathrm{b}}{\omega_\mathrm{b} I_\mathrm{b}} = \frac{U_\mathrm{N}/\sqrt{3}}{\omega_\mathrm{N} I_\mathrm{N}},$$

$$S_\mathrm{b} = \sqrt{3}U_\mathrm{N} I_\mathrm{N},$$

$$\psi_\mathrm{b} = \frac{U_\mathrm{b}}{\omega_\mathrm{b}} = \frac{\sqrt{2}U_\mathrm{N}/\sqrt{3}}{\omega_\mathrm{N}},$$

$$T_\mathrm{b} = \frac{3}{2}p_\mathrm{N}\psi_\mathrm{b} I_\mathrm{b} = \frac{3I_\mathrm{N}U_\mathrm{N}/\sqrt{3}}{\omega_\mathrm{N}/p_\mathrm{N}}.$$

Transmission from the per unit values to real values are done with following equations

$$u = u_\mathrm{pu} U_\mathrm{b},$$

$$i = i_\mathrm{pu} I_\mathrm{b},$$

$$R = r_\mathrm{pu} Z_\mathrm{b},$$

$$L = l_\mathrm{pu} L_\mathrm{b},$$

$$\psi = \psi_\mathrm{pu}\psi_\mathrm{b},$$

$$T = t_{\mathrm{pu}} T_{\mathrm{b}}.$$

On the previous equations following parameters are used:

The rated values of the machine

U_{N}	rated voltage (line-to-line)
I_{N}	rated current
f_{N}	rated frequency
ω_{N}	rated angular frequency
p_{N}	pole pair number

Base values

U_{b}	voltage, normally selected to U_{N}
I_{b}	current, normally selected to I_{N}
ω_{b}	angular frequency, normally selected to ω_{N}
L_{b}	inductance
ψ_{b}	flux linkage
T_{b}	torque

Per unit values of the parameters

u_{pu}	voltage
i_{pu}	current
r_{pu}	resistance
l_{pu}	inductance
ψ_{pu}	flux linkage
t_{pu}	torque

Real values of the parameters

u	voltage
i	current
R	resistance
L	inductance
ψ	flux linkage

T torque